FLUID-TO-PARTICLE HEAT TRANSFER IN A VERTICAL MOVING BED OF SOLIDS WITH INTERSTITIAL FLUID FLOW

A THESIS

Presented to

The Faculty of the Graduate Division

by

Leighton Esten Sissom

In Partial Fulfillment

of the Requirements for the Degree

Doctor of Philosophy in the

School of Mechanical Engineering

Georgia Institute of Technology

June, 1965

FLUID-TO-PARTICLE HEAT TRANSFER

IN A VERTICAL MOVING BED OF SOLIDS

WITH INTERSTITIAL FLUID FLOW

Approved:

Chairman

Date approved by Chairman: May 18, 1965

ACKNOWLEDGMENTS

The author is very grateful to the many people who have encouraged him throughout his life. Without their understanding and assistance his educational endeavor would have been impossible.

To Dr. Thomas W. Jackson, whose enthusiastic guidance has led to the culmination of this work, deep appreciation is expressed. His ability to convey optimism and stimulate action is noteworthy. The constructive comments, the willingness to be helpful, and time given by the members of the thesis committee, Dr. Samuel C. Barnett and Dr. Robin B. Gray, are gratefully acknowledged. A special note of thanks is also due Mr. C. R. Bannister who assisted in the fabrication of the experimental apparatus.

For the guidance in his early life and continued encouragement of his parents the author is indebted. Sincere appreciation goes to his wife, Evelyn, and sons whose endless love and devotion have assisted greatly in reaching this goal.

The author also wishes to express his gratitude to the National Aeronautics and Space Administration for financial assistance which made this undertaking possible.

Finally, the author is grateful above all to God for extending physical and mental blessings throughout his life.

TABLE OF CONTENTS

Page

LIST OF TABLES

LIST OF ILLUSTRATIONS

SUMMARY

The characteristics of non-isothermal two-phase steady flow in a vertical duct of constant area were investigated analytically and experimentally. Small solid particles flowed with gravity while a heated fluid was forced countercurrently to the solids flow. Both portions of the investigation consisted of the determination of the axial temperature distribution of the solids and fluid and other parameters of interest in the performance of a heat exchanger making use of this principle.

Utilizing the regeneration principle, the effective length of a fluid-to-particle heat exchanger was predicted by theory and verified by experiment. Its small value, given for several sets of flow conditions, indicates that such a heat exchanger would be very compact. For the aluminum granules used in this investigation (0.027 in. weight mean diameter) the effective surface area to volume ratio was 2,980 (sq. ft.)/(cu. ft.) which is considerably above the value of 200 that is usually taken as the lower limit for a compact heat exchanger. Due to the large contact area in a relatively small volume of particles the heat transfer rate may be increased considerably, without changing the heat transfer coefficient or the thermal driving force, by simply decreasing the size of the particles.

For the analytical portion of this study the governing equations were determined by making an energy balance on all of the material, both solid and fluid, and on the solid alone. There were five simultaneous mechanisms for heat flow; namely, conduction through the solid particles, conduction through the continuous media, enthalpy transport of the solids and the fluid, and

convective transfer between the fluid and the solid particles through a film resistance. Second order differential equations resulted, and a closed form solution was obtained. The analysis showed that beyond the effective length mentioned above no heat is transferred, and both solids and fluid remain at a constant temperature throughout any further length which the regenerator may have. It was necessary to determine the effective length by trial and error since the flow conditions were so complexly related to the boundary conditions. In general, previous investigators have assumed that the temperature of the solids essentially remains constant; however, this analysis has shown an exponential variation but less pronounced than that of the fluid.

In the experimental investigation the solids flow rate and the fluid (air) flow rate were varied independently in order to provide more flexible experimental capabilities. The void fraction varied less than four per cent for the range tested; but, for a practical regenerator, the solids should be constrained to move in a "dense swarm" since the effective thermal conductivity varies with the void fraction. Pressure differentials were low enough that such a system may be applicable to a turbine-powered mobile vehicle.

NOMENCLATURE

a	constant, Appendix B
A	area, sq. ft.
b	constant, Appendix B
c	specific heat, Btu/(lbm-°R)
$C_1, \cdots, C_8$	integration constants; equations (2.4), (2.6), (2.11) and (2.14)
d	average sieve diameter, ft.
$\frac{d_t}{d_p}$	tube to particle diameter ratio
D_p	weight mean diameter, $\sum wd$, ft.
e	eddy diffusivity, ft./hr.
E	$(1 - \frac{m_1^2}{\lambda} - \frac{\beta m_1}{\lambda})$
f	constant; equations (4.3) and (4.4)
F	$(1 - \frac{m_2^2}{\lambda} - \frac{\beta m_2}{\lambda})$
g	constant; equations (4.3) and (4.4)
G	$(1 - \frac{m_3^2}{\lambda} - \frac{\beta m_3}{\lambda})$
$G_{( )}$	ρV, mass velocity, lbm/(sq. ft. -hr.)
h	convective film coefficient, Btu/(hr. -sq. ft. -°R)
$h_{( )}$	enthalpy, Btu/lbm
J	$e^{m_1 L_e}$
k	thermal conductivity, Btu/(hr. -ft. -°R)

K	$e^{m_2 L_e}$
L	length of heat exchanger, ft.
m_1, m_2, m_3	roots; equations (2.8), (2.9), and (2.10)
N	$e^{m_3 L_e}$
N_{Pr}	Prandtl number
p	constant, Appendix B
q	constant, Appendix B
q''	heat flux, Btu/(hr.-sq.ft.)
r	constant, Appendix B
$\underline{r}$	space coordinate
R	duct radius, ft.
S	effective surface area, sq.ft.
S'''	$\frac{S}{\Delta \underline{V}}$, (sq.ft.)/(cu.ft.)
T	temperature, °R
T_o	ambient temperature, °F
U	$m_1 J$
v	specific volume, (cu.ft.)/lbm
V	$m_2 K$
$V_{( )}$	velocity, fps
$\underline{V}$	volume, cu.ft.
w	weight percentage of particles of average sieve diameter d
W	$m_3 N$
z	space coordinate
$\overline{( )}$	average value

Subscripts

1	pure continuous phase in two-phase flow
2	pure discontinuous phase in two-phase flow
e	effective
f	fluid
o	superficial
p	constant pressure
s	solid
t	turbulent

Greek Symbols

α	$\dfrac{\epsilon \bar{k}_f}{(1-\epsilon) k_{s,e}}$
$\left(\dfrac{\alpha_s}{\alpha_v}\right)$	material constant, Appendix D
β	$(-) \dfrac{G_s c_s}{k_{s,e}}$
δ	particle roughness factor
Δ	finite increment
ϵ	void fraction, (void volume)/(total volume)
η	$(-) \dfrac{G_{f_o} \bar{c}_{pf}}{(1-\epsilon) k_{s,e}}$
θ	space coordinate
λ	$\dfrac{hS'''}{(1-\epsilon) k_{s,e}}$
μ	dynamic viscosity, lbm/(hr. -ft.)

ν	kinematic viscosity, (sq. ft.)/hr.
ξ, ξ_1, ξ_2	functions
ρ	density, lbm/(cu. ft.)
φ	angle in trigonometric solution of cubic equation; equation (B. 7)
Ψ	particle shape factor

CHAPTER I

INTRODUCTION AND HISTORICAL BACKGROUND

The flow of solid particles within a fluid has been of interest since man first observed dust, twigs, and other small particles being lifted and carried about by the wind. A study of this phenomenon falls logically into three categories: (a) fixed bed, (b) fluidized bed, and (c) moving bed. These categories, depicted graphically in Figure 1 for vertical cogravity solids flow and countercurrent fluid flow, have the following distinguishing characteristics:

(a) Fixed bed: The solid particles remain fixed, being restrained by porous screens, while the fluid is passed through the bed of particles.

(b) Fluidized bed: The solid particles are unrestrained at the top and the bed expands as the fluid velocity increases. There is no net solids flow.

(c) Moving bed: In this case both solids and fluid flow. Obviously then, the relative velocity is of importance, and the effects produced by this relative motion lead to complexities which have not been completely understood or analyzed.

The intent of this study is to investigate the case of the moving bed as it applies to a regenerative-type heat exchanger. In the ordinary recuperator-type heat exchanger two fluids are separated by walls which prevent their mixing at the expense of resisting the flow of heat across two films and a wall.

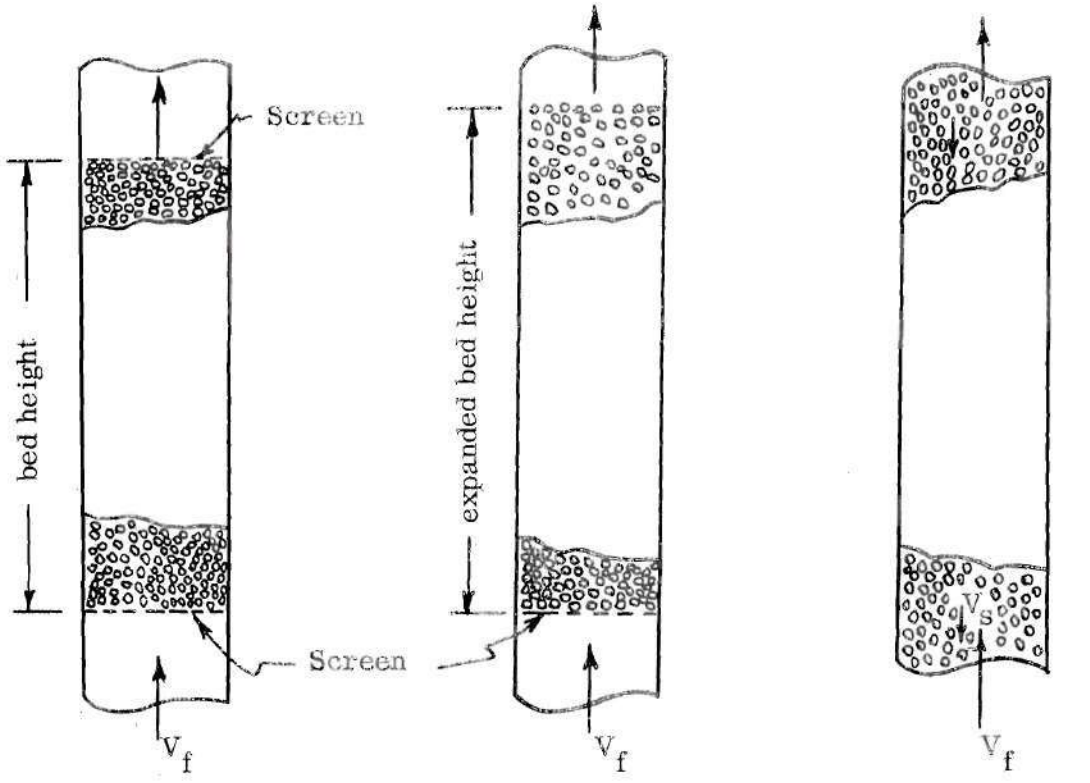

(a) Fixed Bed (b) Fluidized Bed (c) Moving Bed

Figure 1. Two-Phase Flow Systems

However, in a regenerator the heat is generally exchanged between solid particles and a fluid. Two units are usually used through which hot and cold fluids flow alternately in order to have continuous operation (1). By permitting the solid particles to flow, i.e., regenerating them, only one unit is necessary.

The analytical portion of this study is based upon five simultaneous mechanisms for heat flow. These are conduction through the solid particles, conduction through the continuous media, enthalpy transport of solids and fluid, and heat flow between the fluid and particles through a film resistance. The results permit the initial design length to be predicted for a compact regenerative heat exchanger, which may find application, for example, in turbine powered mobile vehicles presently being developed.

Moving bed techniques have been applied successfully in the transport of coal, chemicals, and various slurries in the chemical, mining, and food processing industries. Many of these operations are basically isothermal and most studies have been primarily concerned with the velocity field, boundary stresses, and physical properties.

Related Literature Survey

In their classical paper of 1924 Cramp and Priestly (2) outlined the main principles of the vertical pumping of grain. Chatley (3) extended this work by including some of the previously neglected parameters. Davis (4) contributed also to this early work on the concurrent flow of solids and fluid. The same principles were utilized in studies of the hydraulic transport of solids (5, 6, 7).

A rather extensive investigation of moving, isothermal, vertical beds was conducted at Princeton University (8, 9, 10, 11, 12) from which a

relatively new technique for fluid-particle contacting was recognized for an incompressible fluid. The concept of slip velocity, defined as the difference between the net fluid and particle velocities, was amplified.

Delaplaine (13) presents the results of a study of the stresses acting in beds of noncohesive granular solids flowing under steady state conditions in vertical vessels in a stagnant atmosphere. Nine years of study and experimentation at the University of Utah (14, 15) yielded considerable data on the gravity flow of solids; however, this was also for isothermal systems and it was in a stagnant atmosphere.

An excellent comprehensive survey of fluidization and fluid-particle systems is contained in a reference book by Zenz and Othmer (16), but very little is said about fluid-to-particle heat transfer in moving systems. At a 1962 London symposium on the interaction between fluids and particles (17) a paper was presented on heat transfer in moving beds based upon the joint probability-distribution of a particle being in two given places at two given times.

In the non-isothermal cases wall-to-moving bed heat transfer has been investigated quite thoroughly experimentally and to a lesser extent analytically due to the complicated mechanism (18, 19, 20, 21). Fluid-to-particle heat transfer has been investigated even less and primarily empirically. A summary of investigations made over a decade is presented by Frantz (22) where film coefficients are presented as a function of the flow parameters for both gases and liquids. The recommended correlation given for predicting apparent fluid-to-particle heat transfer coefficients when fluid temperatures are measured with bare thermocouples is:

$$\frac{hD_p}{k_f} = 0.016 \left(\frac{D_p G}{\mu_f}\right)^{1.3} \left(\frac{c_{pf}\mu_f}{k_f}\right)^{0.67} \qquad (1.1)$$

This form is similiar to that which is usually used for correlating forced convection heat transfer coefficients. It seems reasonable that the mass velocity parameter must include the relative velocity, i.e., $G = \rho_f(V_f - V_s)$. The transport properties are evaluated at the mean bulk fluid temperature and D_p is the weight mean diameter (16). More recently (September 1964) Fujishige (23, 24) reported film coefficients for both wall-to-bed and fluid (air)-to-particle heat transfer.

Kunii (25) and Yagi and Kunii (26) summarize effective thermal conductivities in packed beds with flowing gases. Analytical expressions and a summary of experimental values are given by Gorring and Churchill (27) for the thermal conductivity of heterogeneous materials. Bernard and Wilhelm (28) studied turbulent diffusion in beds of packed solids through which a fluid flowed. Their presentation included a limited number of values of eddy diffusivity, e, to be used to find the effective thermal conductivity of the fluid when turbulence is present by use of the equation

$$(k_f)_{eff} = k_f + k_t = k_f + \rho_f c_{pf} e \qquad (1.2)$$

Munro and Amundson (29) considered heat exchange between solid and fluid in moving beds, but they neglected the conduction in the fluid in the direction of flow.

CHAPTER II

ANALYTICAL INVESTIGATIONS

Mathematical Statement of the Problem

The system of this investigation is made up of a heterogeneous network of pores and solid particles (Figure 1,c). The solid particles move downward under the influence of gravity with velocity V_s. The fluid moves either upward or downward, due to a static pressure differential, at velocity V_f. When the fluid moves upward the particle motion is retarded (may be stopped or even reversed depending upon the flow rate), but upon moving downward the particle velocity is increased.

At the wall one can expect the no-slip condition to apply to the fluid in the voids; however, the "scrubbing action" of the solids disrupts this condition where the solids come in contact with the wall. Also the solids touching the wall may slip or roll depending upon the environmental forces and friction coefficients. For the case of dense solids, as in this investigation, these mentioned effects taken together cause both solids and fluid to move as a slug except for an extremely thin boundary layer (30). Of course, this boundary layer thickness depends primarily upon the size of the particles, being of the same order as the particle diameter. The error introduced by neglecting the boundary layer depends upon the tube diameter to particle diameter ratio d_t/d_p. As d_t/d_p increases the error is reduced and is generally neglected when $d_t/d_p \geq 10$ (31).

For $d_t/d_p \lesssim 8$ it may be pointed out that the fluid velocity profile may be as indicated in Figure 2 due to a difference in voidage at points A and B.

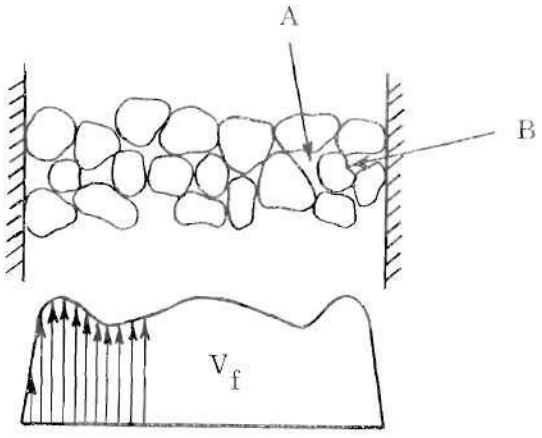

Figure 2. Possible Velocity Profile for $d_t/d_p \lesssim 8$

As a result of the preceeding arguments, average values for both solid and fluid velocity will be used in this analysis. For the d_t/d_p ratio in this investigation it is believed that these average values approximate very closely the actual values.

In studying the pressure drop through packed beds numerous investigators have used two approaches in general. One method is to regard the particles as submerged objects. Then the pressure drop is given by the sum of the resistances of the collection of particles. The other method considers the column as being made up of a bundle of tubes of weird cross-section. The theory for uniform straight tubes is then modified to apply. With the proper evaluation of effective parameters it is believed that either approach may be taken in a heat transfer investigation. A modification of the second method will be considered.

By making an energy balance on all of the material, both solid and fluid, and on the solid alone, respectively, the following differential equations result (see Appendix A).

$$\frac{d^2T_s}{dz^2} + \frac{\epsilon \bar{k}_f}{(1-\epsilon)k_{s,e}} \frac{d^2T_f}{dz^2} - \frac{G_s c_s}{k_{s,e}} \frac{dT_s}{dz} - \frac{G_{fo} c_{pf}}{(1-\epsilon)k_{s,e}} \frac{dT_f}{dz} = 0 \qquad (2.1)$$

$$\frac{d^2T_s}{dz^2} - \frac{G_s c_s}{k_{s,e}} \frac{dT_s}{dz} + \frac{hS'''}{(1-\epsilon)k_{s,e}} (T_f - T_s) = 0 \qquad (2.2)$$

Effective Length

Because of the smallness of the particles and their high thermal conductivity, their temperature will approach the gas temperature very rapidly. Consider the case of cold solids flowing downward while hot gas flows upward, i.e., $(T_s)_{in} < (T_f)_{in}$. There is then an intermediate point, i, where $T_s \cong T_f$. Consider the two regimes as indicated in Figure 3 and define the following for convenience.

$$\alpha \equiv \frac{\epsilon \bar{k}_f}{(1-\epsilon)k_{s,e}}$$

$$\beta \equiv (-) \frac{G_s c_s}{k_{s,e}}$$

$$\eta \equiv (-) \frac{G_{fo} \bar{c}_{pf}}{(1-\epsilon) k_{s,e}}$$

$$\lambda \equiv \frac{hS'''}{(1-\epsilon)k_{s,e}}$$

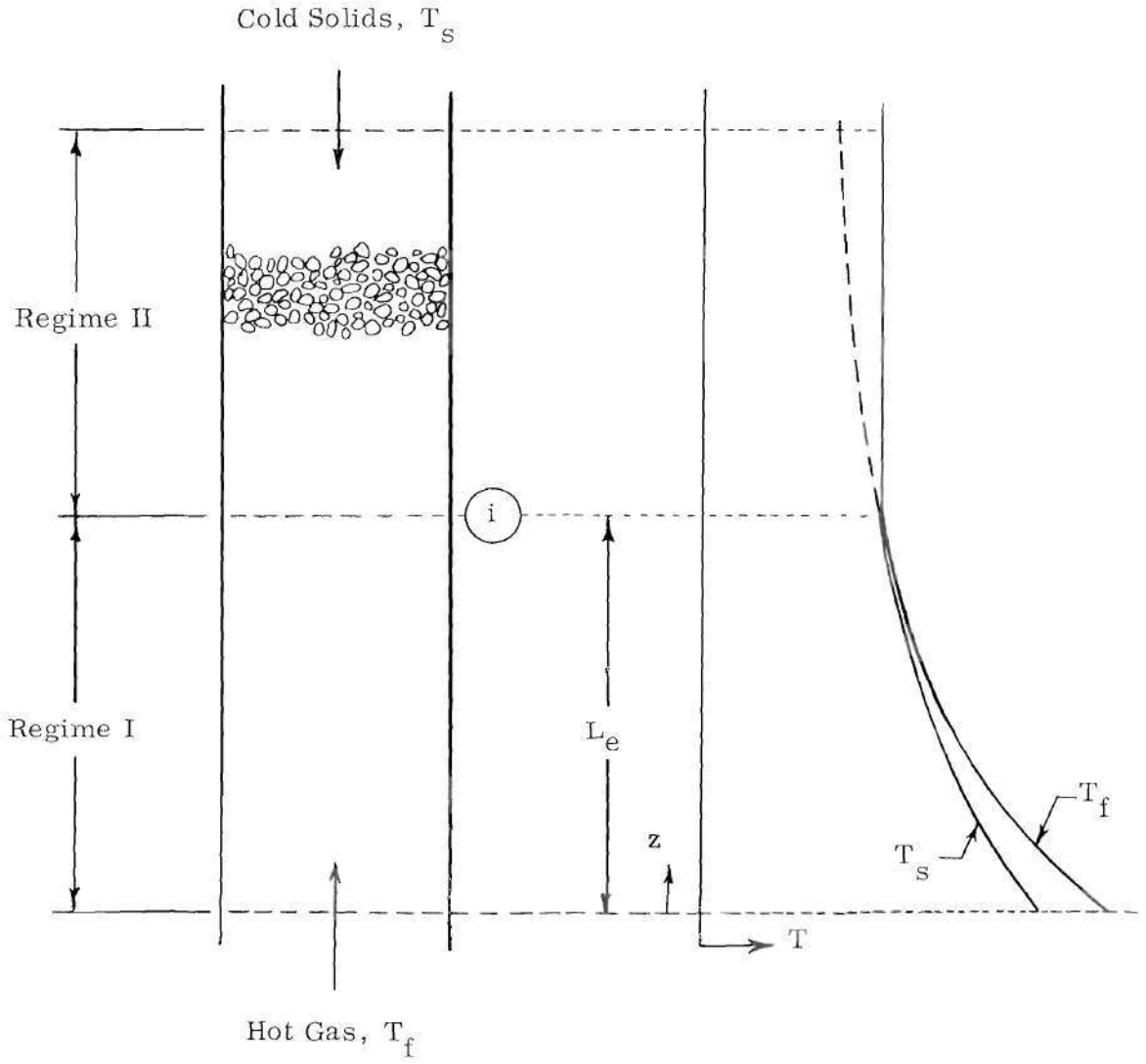

Figure 3. Definition of Effective Length

$$\bar{c}_{pf} \equiv \frac{\int_a^z c_{pf} dT}{T_{f_z} - T_{fa}}$$

Equations (2.1) and (2.2) become respectively:

$$\frac{d^2T_s}{dz^2} + \alpha \frac{d^2T_f}{dz^2} + \beta \frac{dT_s}{dz} + \eta \frac{dT_f}{dz} = 0 \qquad (2.1a)$$

$$\frac{d^2T_s}{dz^2} + \beta \frac{dT_s}{dz} + \lambda (T_f - T_s) = 0 \qquad (2.2a)$$

Considering first Regime II ($T_f = T_s$), from equation (2.1a) the following is obtained:

$$(1 + \alpha) \frac{d^2T_f}{dz^2} + (\beta + \eta) \frac{dT_f}{dz} = 0 \qquad (2.3)$$

which has the solution:

$$T_f = C_1 e^{-\left(\frac{\beta + \eta}{1 + \alpha}\right)z} + C_2 \qquad (2.4)$$

Equation (2.2a) gives,

$$\frac{d^2T_s}{dz^2} + \beta \frac{dT_s}{dz} = 0 \tag{2.5}$$

with the solution:

$$T_s = C_3 e^{-\beta z} + C_4 \tag{2.6}$$

Now by the condition postulated in Regime II, i.e., $T_s = T_f$, equations (2.4) and (2.6) can only be true if $C_1 = C_3 = 0$ since $(\beta + \eta)/(1 + \alpha) \neq \beta$. That is, the temperature is a constant, $C_2 = C_4$, in Regime II. In other words, the heat is transferred completely in Regime I where convection is the predominate mode.

Using the method of operators, where $D \equiv d(\ )/dz$, equations (2.1a) and (2.2a) for Regime I may be written as:

$$(D^2 + \beta D) T_s + (\alpha D^2 + \eta D) T_f = 0 \tag{2.1b}$$

$$(D^2 + \beta D - \lambda) T_s + \lambda T_f = 0 \tag{2.2b}$$

Multiplying equation (2.1b) by λ, operating on equation (2.2b) with $(\alpha D^2 + \eta D)$, and subtracting gives:

$$\lambda(D^2 + \beta D) T_s - (\alpha D^2 + \eta D)(D^2 + \beta D - \lambda) T_s = 0 \tag{2.7}$$

$$\text{or,}\quad D\left(D^3 + \left[\beta + \frac{\eta}{\alpha}\right]D^2 - \left[\frac{\lambda(\alpha+1) - \beta\eta}{\alpha}\right]D - \left[\frac{\lambda(\beta+\eta)}{\alpha}\right]\right)T_s = 0 \qquad (2.7a)$$

Let

$$p \equiv \beta + \frac{\eta}{\alpha}$$

$$q \equiv -\left[\frac{\lambda(\alpha+1) - \beta\eta}{\alpha}\right]$$

$$r \equiv -\frac{\lambda(\beta+\eta)}{\alpha}$$

Therefore, equation (2.7a) becomes:

$$D(D^3 + pD^2 + qD + r)T_s = 0 \qquad (2.7b)$$

By eliminating T_s between equations (2.1b) and (2.2b) it can easily be shown that a solution for T_f has the same form as one for T_s. The boundary conditions for the two equations separate the resulting curves.

By considering the equivalent algebraic expression for the cubic portion of equation (2.7b) it is shown in Appendix B that there are three real and unequal roots given by:

$$m_1 = 2\sqrt{-\frac{a}{3}}\cos\frac{\varphi}{3} - \frac{p}{3} \qquad (2.8)$$

$$m_2 = 2\sqrt{-\frac{a}{3}}\cos\left(\frac{\varphi}{3} + \frac{2\pi}{3}\right) - \frac{p}{3} \qquad (2.9)$$

$$m_3 = 2\sqrt{-\frac{a}{3}}\cos\left(\frac{\varphi}{3} + \frac{4\pi}{3}\right) - \frac{p}{3} \tag{2.10}$$

The solution of equation (2.7b) is therefore:

$$T_s = C_5 + C_6 e^{m_1 z} + C_7 e^{m_2 z} + C_8 e^{m_3 z} \tag{2.11}$$

Differentiating equation (2.11),

$$\frac{dT_s}{dz} = C_6 m_1 e^{m_1 z} + C_7 m_2 e^{m_2 z} + C_8 m_3 e^{m_3 z} \tag{2.12}$$

$$\frac{d^2T_s}{dz^2} = C_6 m_1^2 e^{m_1 z} + C_7 m_2^2 e^{m_2 z} + C_8 m_3^2 e^{m_3 z} \tag{2.13}$$

Solving equation (2.2a) for T_f and using equations (2.11), (2.12), and (2.13),

$$T_f = T_s - \frac{1}{\lambda}\frac{d^2T_s}{dz^2} - \frac{\beta}{\lambda}\frac{dT_s}{dz}$$

$$T_f = C_5 + C_6\left(1 - \frac{m_1^2}{\lambda} - \frac{\beta m_1}{\lambda}\right)e^{m_1 z} + C_7\left(1 - \frac{m_2^2}{\lambda} - \frac{\beta m_2}{\lambda}\right)e^{m_2 z}$$

$$+ C_8\left(1 - \frac{m_3^2}{\lambda} - \frac{\beta m_3}{\lambda}\right)e^{m_3 z} \tag{2.14}$$

Utilizing the following boundary conditions in equations (2.11) and (2.14) the arbitrary constants may be determined.

(a) at $z = 0$: $T_f = (T_f)_{in}$

(b) at $z = L_e$: (i) $T_s = (T_s)_{in}$; $dT_s/dz = 0$; $dT_f/dz = 0$

(ii) $(T_f)_{out} \cong (T_s)_{in}$

It may be observed that L_e is not a fixed length until the flow conditions and temperature differential are specified. This requires the "additional boundary condition."

The following are defined for convenience in subsequent calculation.

$$E \equiv \left(1 - \frac{m_1^2}{\lambda} - \frac{\beta m_1}{\lambda}\right)$$

$$F \equiv \left(1 - \frac{m_2^2}{\lambda} - \frac{\beta m_2}{\lambda}\right)$$

$$G \equiv \left(1 - \frac{m_3^2}{\lambda} - \frac{\beta m_3}{\lambda}\right)$$

Differentiating equation (2.14) and applying boundary condition (a) to equation 2.14,

$$\frac{dT_f}{dz} = C_6 E m_1 e^{m_1 z} + C_7 F m_2 e^{m_2 z} + C_8 G m_3 e^{m_3 z} \qquad (2.15)$$

$$(T_f)_{in} = C_5 + EC_6 + FC_7 + GC_8 \qquad (2.16)$$

From boundary condition (b,i) and equations (2.11), (2.12), and (2.15)

$$(T_s)_{in} = C_5 + C_6 e^{m_1 L_e} + C_7 e^{m_2 L_e} + C_8 e^{m_3 L_e} \tag{2.17}$$

$$0 = C_6 m_1 e^{m_1 L_e} + C_7 m_2 e^{m_2 L_e} + C_8 m_3 e^{m_3 L_e} \tag{2.18}$$

$$0 = C_6 E m_1 e^{m_1 L_e} + C_7 F m_2 e^{m_2 L_e} + C_8 G m_3 e^{m_3 L_e} \tag{2.19}$$

To simplify further let

$$J \equiv e^{m_1 L_e}$$

$$K \equiv e^{m_2 L_e}$$

$$N \equiv e^{m_3 L_e}$$

$$U \equiv m_1 e^{m_1 L_e}$$

$$V \equiv m_2 e^{m_2 L_e}$$

$$W \equiv m_3 e^{m_3 L_e}$$

and rearrange into "standard form."

$$C_5 + EC_6 + FC_7 + GC_8 = (T_f)_{in} \tag{2.16a}$$

$$C_5 + JC_6 + KC_7 + NC_8 = (T_s)_{in} \tag{2.17a}$$

$$UC_6 + VC_7 + WC_8 = 0 \tag{2.18a}$$

$$EUC_6 + FVC_7 + GWC_8 = 0 \tag{2.19a}$$

Since the determinant of the coefficients does not vanish Cramer's rule may be used to solve. Let

$$D \equiv \begin{vmatrix} 1 & E & F & G \\ 1 & J & K & N \\ 0 & U & V & W \\ 0 & EU & FV & GW \end{vmatrix}$$

$$D_5 = \begin{vmatrix} (T_f)_{in} & E & F & G \\ (T_s)_{in} & J & K & N \\ 0 & U & V & W \\ 0 & EU & FV & GW \end{vmatrix}$$

$$D_6 \equiv \begin{vmatrix} 1 & (T_f)_{in} & F & G \\ 1 & (T_s)_{in} & K & N \\ 0 & 0 & V & W \\ 0 & 0 & FV & GW \end{vmatrix}$$

$$D_7 \equiv \begin{vmatrix} 1 & E & (T_f)_{in} & G \\ 1 & J & (T_s)_{in} & N \\ 0 & U & 0 & W \\ 0 & EU & 0 & GW \end{vmatrix}$$

$$D_8 \equiv \begin{vmatrix} 1 & E & F & (T_f)_{in} \\ 1 & J & K & (T_s)_{in} \\ 0 & U & V & 0 \\ 0 & EU & FV & 0 \end{vmatrix}$$

Then

$$C_5 \equiv D_5/D \tag{2.20}$$

$$C_6 \equiv D_6/D \tag{2.21}$$

$$C_7 \equiv D_7/D \tag{2.22}$$

$$C_8 \equiv D_8/D \tag{2.23}$$

Utilizing these constants the temperature distribution for Regime I for both solids and fluid is given by equations (2.11) and (2.14).

Since the arbitrary constants depend upon the effective length L_e, it was necessary to solve by trial and error utilizing the boundary condition (b,ii). That is, for an assumed value of L_e the arbitrary constants were determined. Then values of T_s and T_f from equations (2.11) and (2.14) were compared. This was continued until $T_s \cong T_f$ after which the temperature profiles may be determined from equations (2.11) and (2.14). In the event that $L < L_e$, $T_s \neq T_f$ when $z = L_e$; however, the equations are still applicable if the appropriate change is made in boundary condition (b). For this analysis it was assumed that $L \geq L_e$.

Typical Theoretical Results

Some reasonable effective parameters were chosen and the temperature profiles were determined by computer. A typical result is shown in Figure 4.

By a careful choice of the effective thermal conductivity of the solids and the film coefficient the temperature profile of the fluid agrees very well with measured values found in the literature. Presently, it is believed that as long as the particles move in "dense swarms" that expressions may be developed for these parameters. These could always be utilized for cocurrent flow; however, they would tend to break down as the particles separate due to excessive counter-current flow. Obviously then, by physically constraining the particles to move in a "dense swarm," this could be circumvented. Heretofore, it has generally been assumed that the solids essentially remain at a constant temperature; however, this analysis has shown the variation to be exponential but less pronounced than that of the fluid.

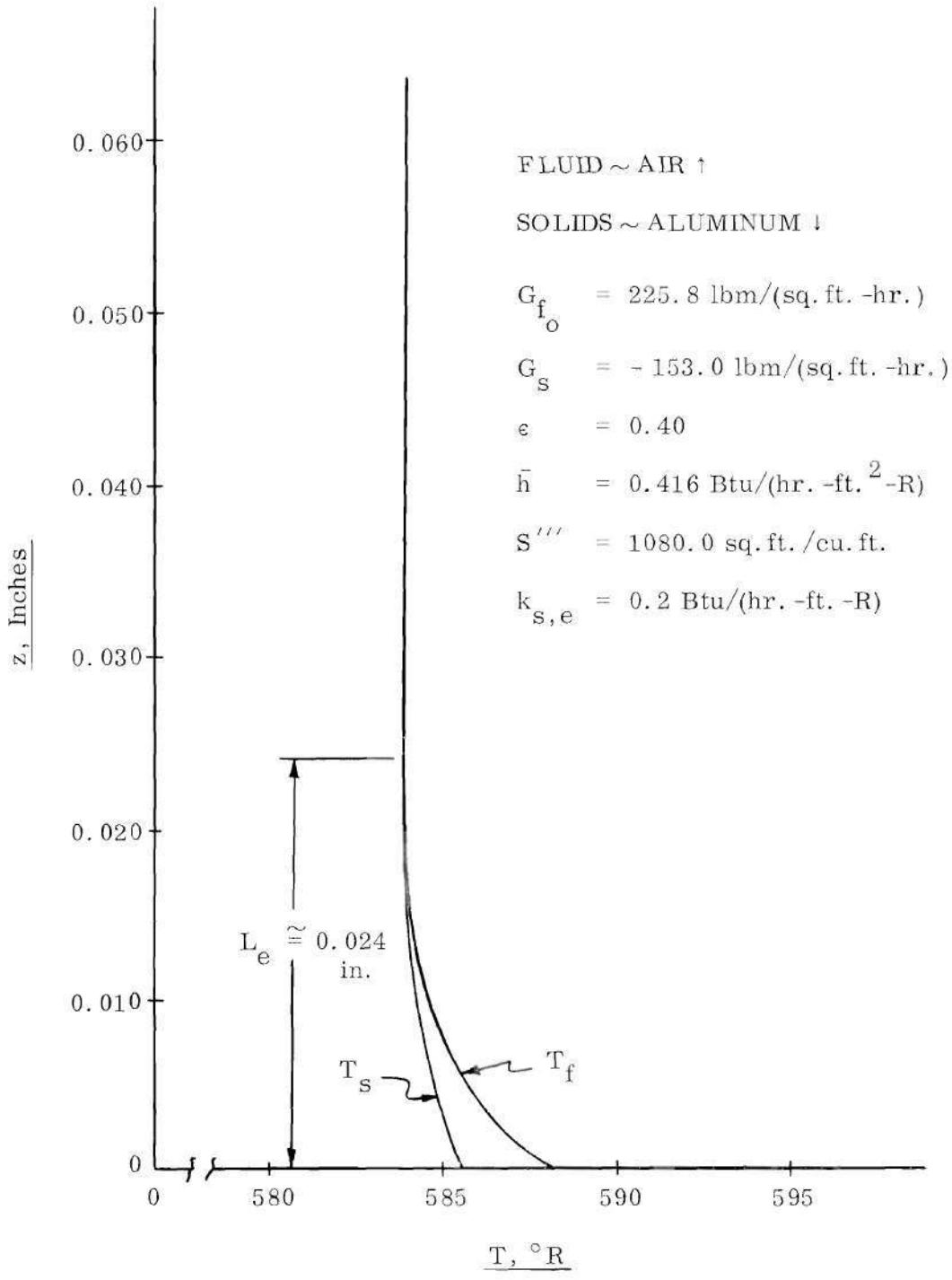

Figure 4. Typical Temperature Distribution

CHAPTER III

EXPERIMENTAL INVESTIGATIONS

Instrumentation and Equipment

The experimental arrangement for this investigation is shown schematically in Figure 5. As can be seen in Figure 6 the main portion of the apparatus was constructed from commercial piping and fittings. It was constructed so that other configurations may be tested in the future if desired; however, only cogravity solids flow with countercurrent fluid flow was considered in this investigation.

Compressed air was brought into the storage bin to facilitate flow of the solid particles by partially fluidizing the bed in the storage bin. This also helped to maintain the solids at a uniform and constant temperature. Solids were permitted to flow into the upper plenum chamber under the action of gravity, and the flow rate was controlled by a W-K-M ACF Industries No. 450 1" Full Port ball valve on the lower end of the test apparatus and the rotary solids feeder which was necessary at low flow rates. A dense swarm of solid particles was maintained throughout the system. Aluminum granules, having the properties given in Appendix D, were used as the regenerated solids.

Filtered compressed air was passed through a bank of three flow meters (F. W. Dwyer Mfg. Co. - Cat. Nos. 500-2, 500-5, 500-9), through the electric resistance heater shown in Figure 7, and into the lower plenum chamber which was equipped with baffles to assure uniform distribution of the heated air. Since it was desired that this metered quantity of air pass upward counter-

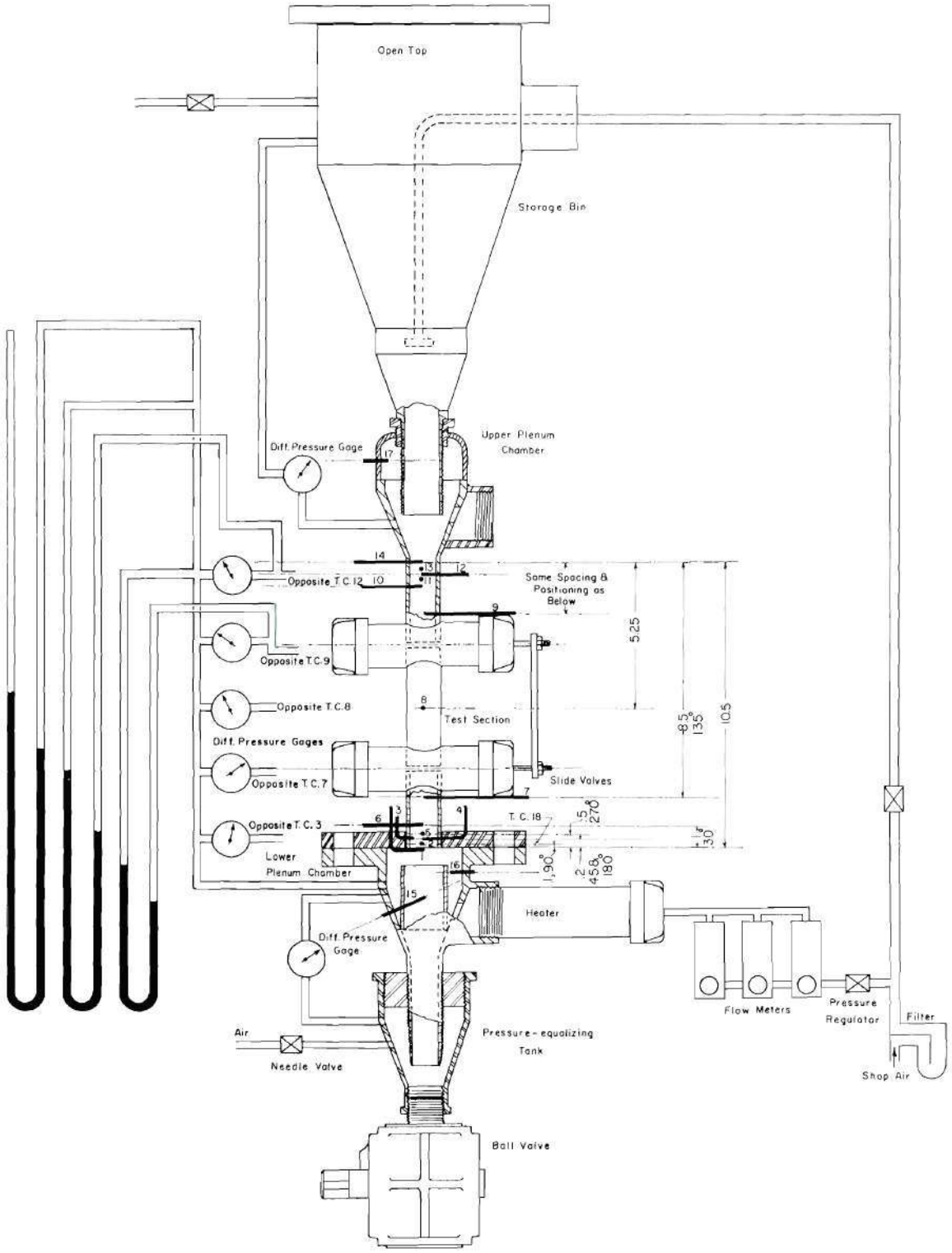

Figure 5. Schematic Diagram of the Experimental Apparatus

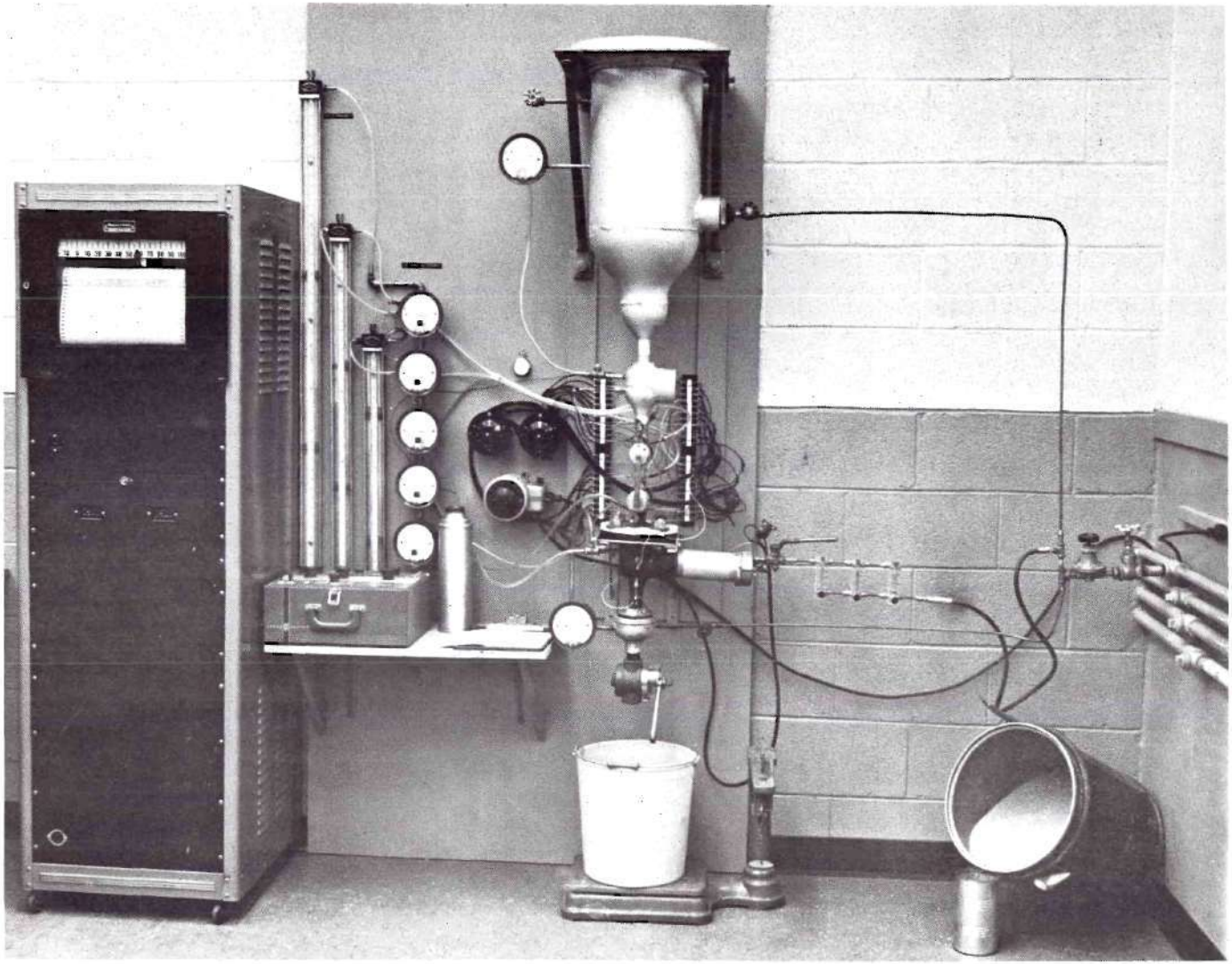

Figure 6. Experimental Apparatus

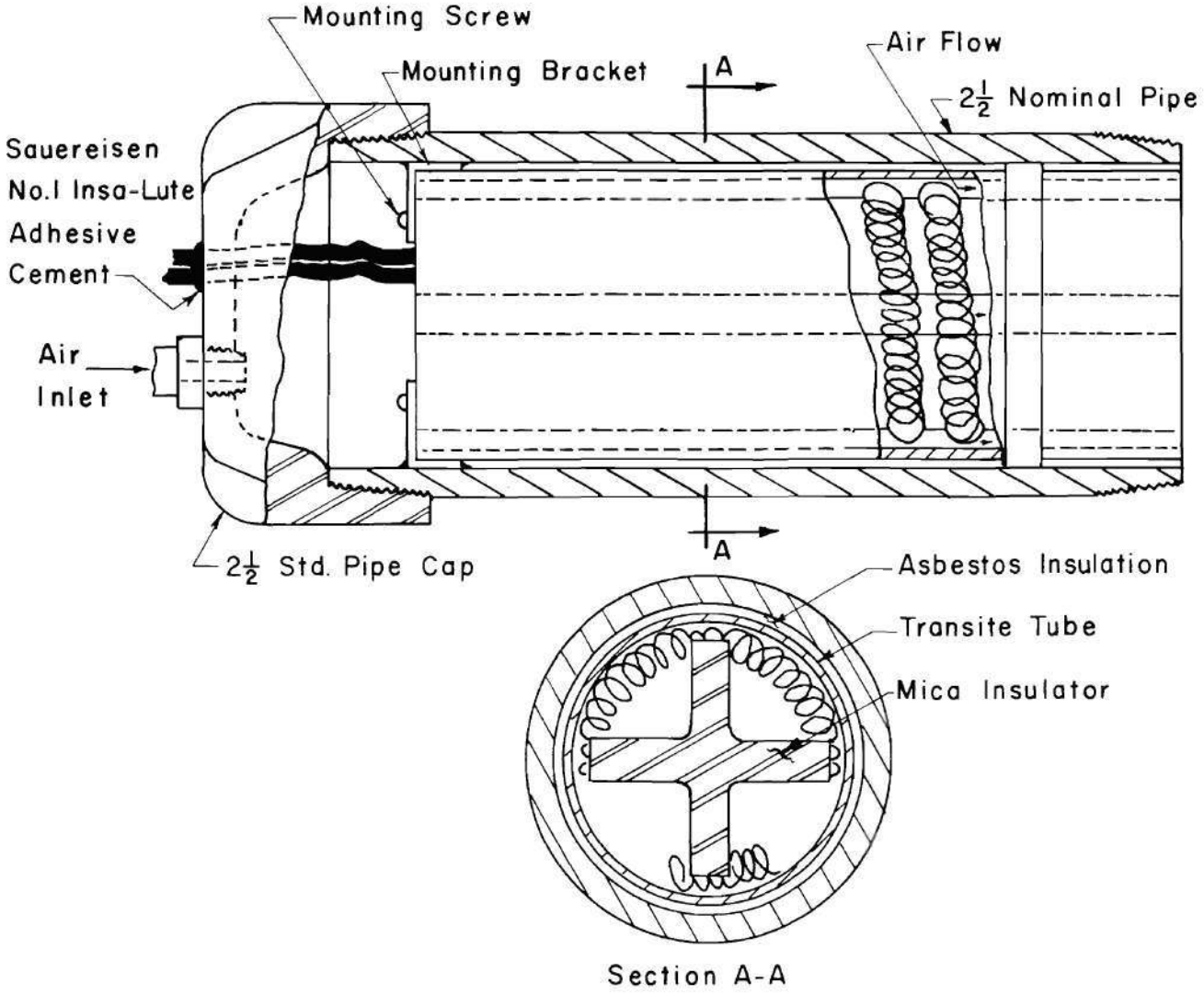

Figure 7. Resistance Heater Detail

current to the moving bed of solids. it was necessary to bring a separate air supply into the pressure-equalizing tank. This air supply was throttled to provide a zero pressure differential between the lower plenum chamber and the pressure-equalizing tank. By utilizing this procedure the metered air passed upward through the one inch nominal diameter test section and spilled to the atmosphere from the upper plenum chamber. The air that was brought into the pressure-equalizing tank passed downward with the flow of solids.

The static pressure in the lower plenum chamber, used for driving the air supply through the test section, was measured by a U-tube manometer. Differential pressures between the lower plenum chamber and various points in the test section were measured by a combination of U-tube manometers and differential pressure gauges (F. W. Dwyer Mfg. Co. - Series 2000 Magnehelic). A Model H-10XT-H Conoflow Corp. pressure regulator was used to prevent pressure surges throughout the system.

Axial temperatures in the test section were sensed by mineral insulated, stainless steel sheathed, chromel-alumel thermocouples (Conax Con-O-Clad SS6K-G-T2) having an outside diameter of 0.062 inch. They were installed radially normal to the test section walls and protruded into the fluid stream. Figure 8 shows their external arrangement. A selector switching system permitted millivolt readings to be made with a No. 8686 Leeds & Northrup Co. Millivolt Potentiometer.

The solids flow rate was determined by weighing the particles that emerged from the system on platform scales (Howe Scale Co. No. 4800) for certain time increments. The time increments were taken of sufficient length that reliable results were obtained. At low flow rates the ball valve would not close sufficiently without clogging. Therefore, it was necessary to build the

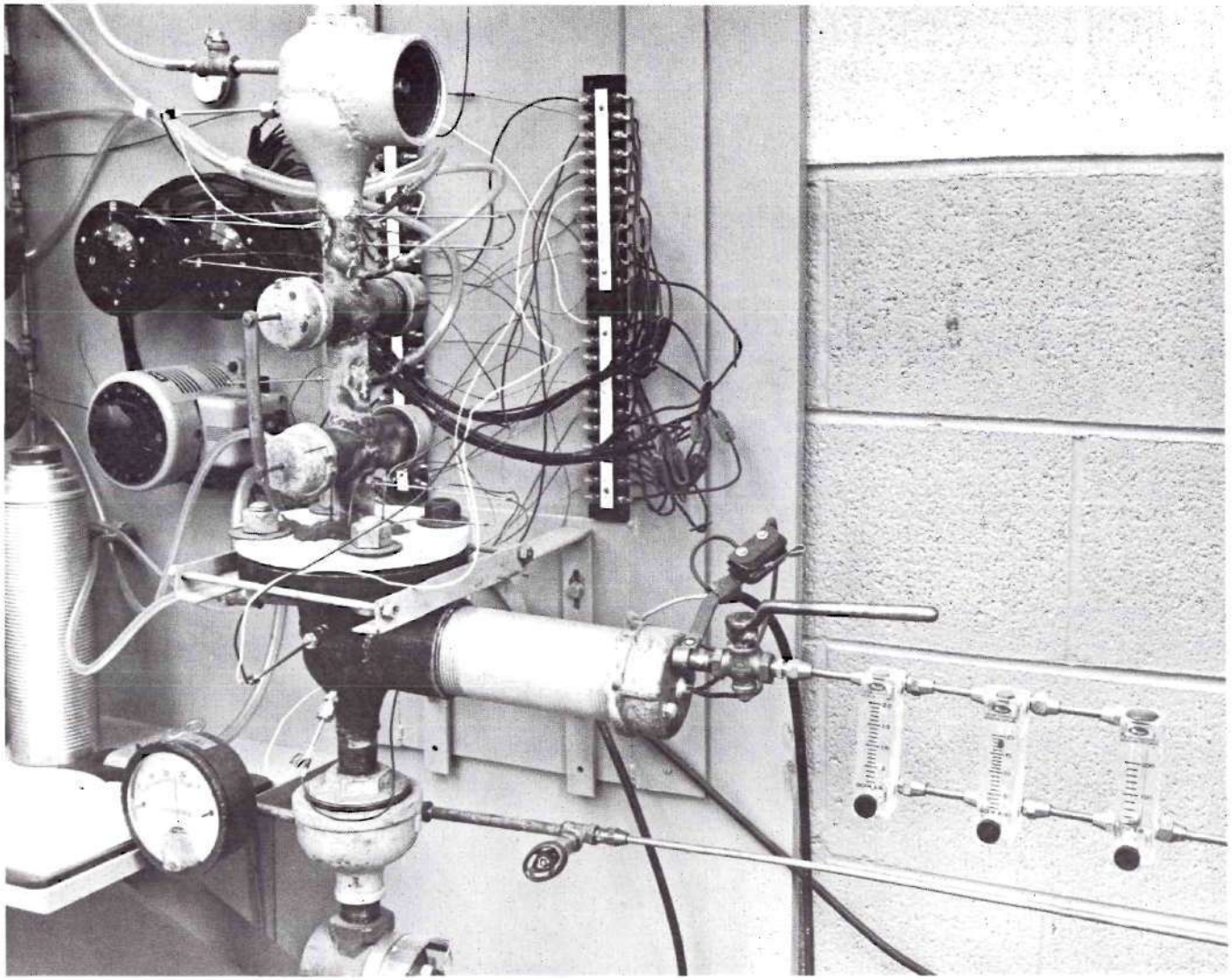

Figure 8. Test Section

rotary solids feeder shown in Figure 9. It was driven through a Vickers Model No. TR3 HR13F13 13 variable speed hydraulic transmission by a General Electric Model No. 5KCP47AB71 electric motor. This permitted solids flow from no-flow to large flow rates to be investigated with very close control; whereas, this was not possible utilizing the ball valve alone.

The heater was equipped with a limit switch, which can be seen in Figure 8, activated by the three-way valve arm in order to de-energize the heater when it was desired to suddenly stop the flow of air through the test chamber as explained in the subsequent section on procedure. The three-way valve permitted the inlet air to be spilled to the surroundings while the limit switch prevented burnout of the heater due to being energized in a stagnant atmosphere. The heater voltage was controlled by a 0-135 volt Powerstat.

To determine the void fraction under flowing conditions slide valves were constructed as shown in Figure 8 (detailed in Figure 10) which could be simultaneously closed by simply pulling the connecting handle. By weighing the solids between the valve gates the void fraction could then be determined, after converting the weight to volume, since the total volume between the gates is known.

After construction, calibration, and trial runs the test column was insulated with Johns-Manville 85% Magnesia pipe insulation and Johns-Manville No. 450 Insulating Cement. The latter is a mineral wool cement with excellent adhesion qualities and was very useful for filling irregular spaces such as around the thermocouples and slide valves. It was also used to seal the magnesia pipe insulation.

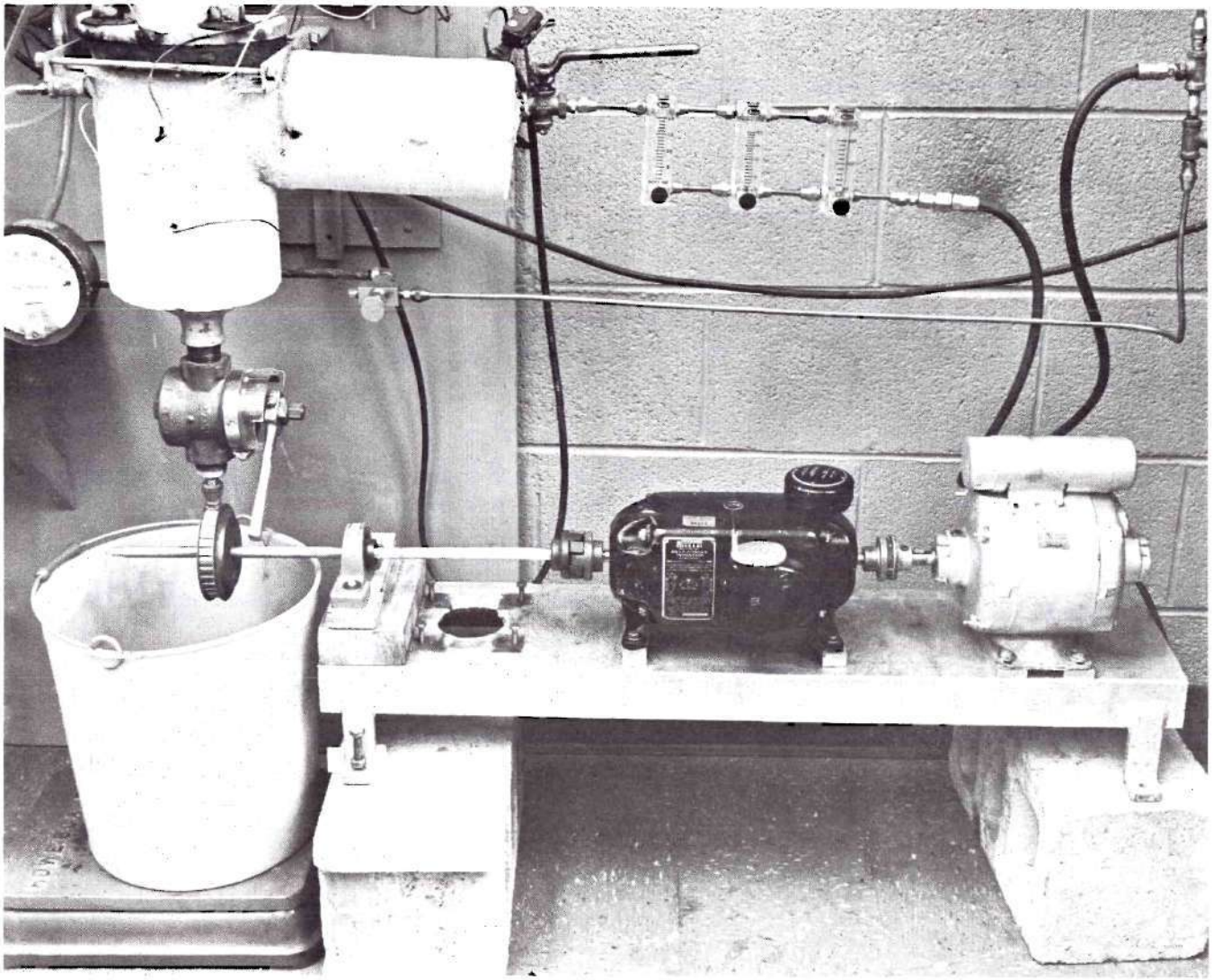

Figure 9. Rotary Solids Feeder

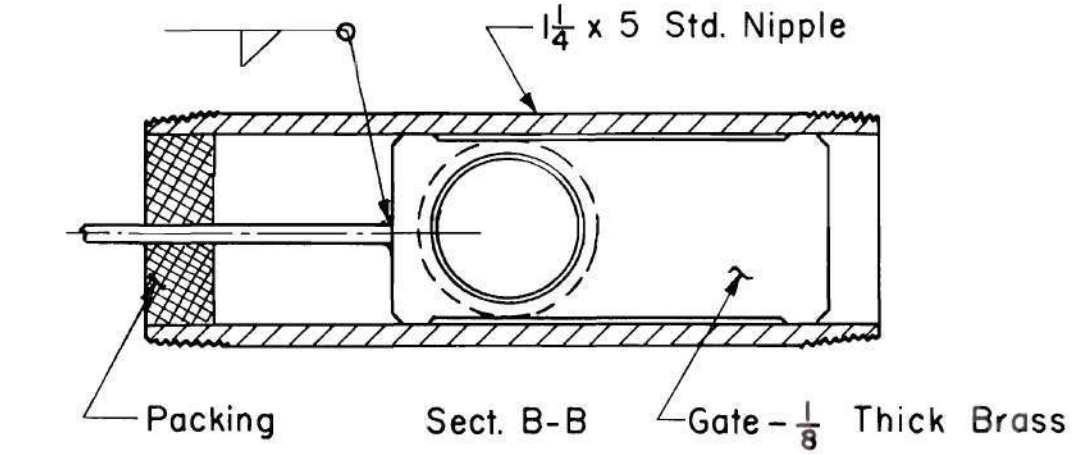

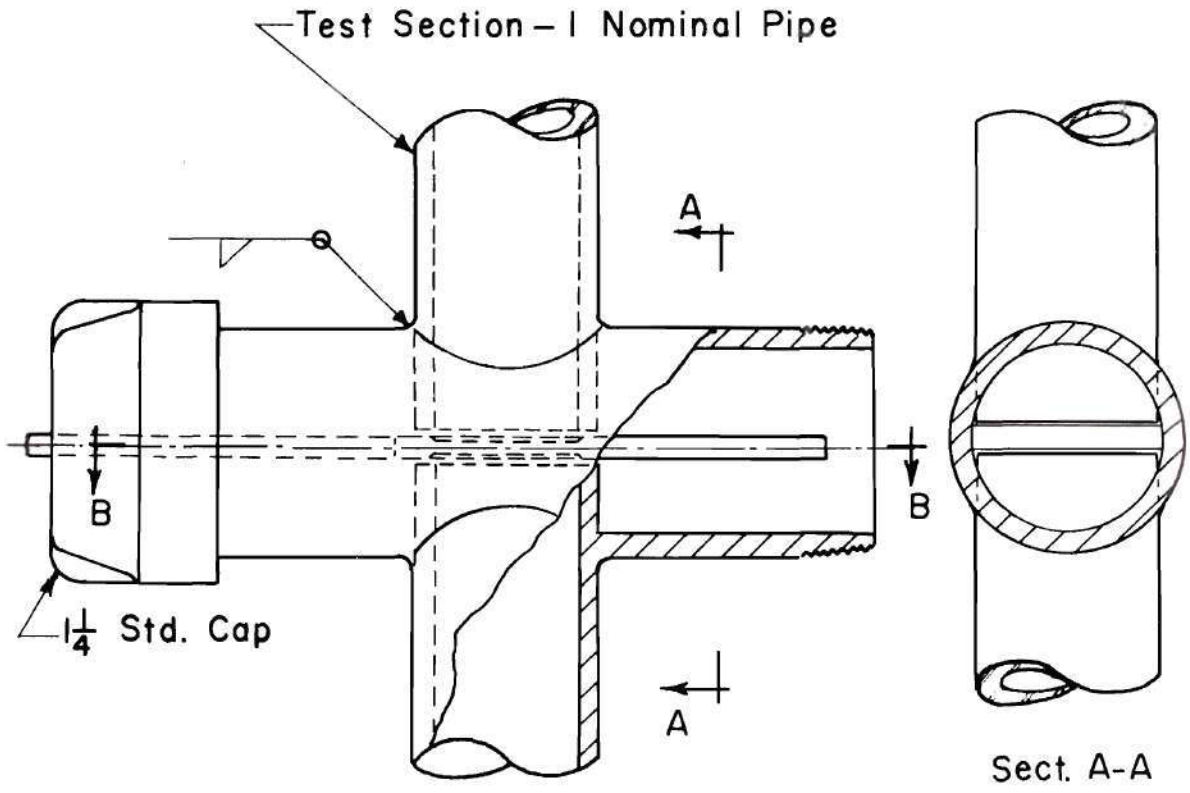

Figure 10. Slide Valve Detail

Experimental Procedure

Because of the large heat capacities of the plenum chambers, test section wall, and various fittings, it was necessary to run the equipment for two or three hours in order for it to reach steady state. Steady state was assumed whenever thermocouple readings along the test section agreed with a set taken several minutes earlier. That is, the system was at least in a "quasi-steady" state for the time interval chosen.

In preparing the apparatus for a series of tests the storage bin was filled with solids and valves were opened permitting a desired rate of air to flow through the flow meters and into the lower plenum chamber through the heater. The heater was then turned on and the voltage was set for a preliminary warmup. During this time the solids valve was closed; therefore, it was necessary to exercise care in keeping the lower plenum chamber pressure low enough to prevent blowout of the manometer fluid.

After preliminary warmup of the hardware the solids valve was opened and the solids feeder was started and set at the desired rate. Air was then throttled into the pressure-equalizing tank to offset the loss of system test air due to opening the solids valve. Adjustments were then made until there was no pressure differential between the lower plenum chamber and the pressure-equalizing tank.

Upon reaching steady state the data presented in tabular form in Appendix C were recorded. During this steady state operation the temperatures indicated by the bare thermocouples were taken as fluid temperatures since Leva (31) has shown that this is very nearly the case. Also, film coefficient equations generally specify that properties are evaluated at the mean bulk temperature measured by bare thermocouples.

Elucidation is required on the measurement of the solids temperature. This, of course, is impossible to do; however, it is believed that a very close approximation was obtained by simultaneously stopping the air and solids flow while taking temperature readings very rapidly. Since the solid particles were then in a stagnant atmosphere and since the thermal conductivity is high and they are small, equilibrium between the stagnant air and the solids was obtained very rapidly. As a matter of fact, it sometimes occurred so rapidly that changes began to take place before all readings were taken. If such occurred, the process was simply restarted, permitted to reach steady state again, and the remainder of the readings were taken upon stopping the air and solids flow as was done previously.

In order not to interfere with other readings, data for determining the void fraction were taken after all other data were recorded. The slide valves were closed and all solids below the lower slide valve gate were permitted to flow from the system. The solid particles trapped between the gates of the slide valves were then released by opening the lower slide valve only. After recording the weight of these particles, the upper slide valve was opened and solids flow was restored. The system could then be changed to new flow conditions for subsequent runs.

Upon shutdown of the operation the heater was first de-energized. Then the solids valve was closed and the rotary feeder was turned off. The air flow into the pressure-equalizing tank was stopped, but air was permitted to continue flowing through the heater until the system was cooled down somewhat. After cooling, all valves were closed; and, water, always a negligible amount, was drained from the filter system. The system was then ready for a subsequent series of tests.

In addition to the actual operation of the system it was further necessary to make a sieve analysis of the aluminum granules used. U. S. Standard Testing Sieves were used and the results are given in Appendix D.

Discussion of Results

Thermocouple T_3, which was installed at the same distance from the entrance as T_2 but displaced from the axis of the test section, indicated that the temperature was essentially uniform over the cross section. The minor deviation may be attributed to entrance effects in the flow pattern, which were caused by the peripheral influx of the air, since it was less pronounced at low air flow rates.

For the runs made without the solids feeder no noticeable effect due to an appreciable change in head of solids in the storage bin was noted, although the head was kept approximately constant. The hopper design and the partial fluidization of the solids bed alleviated this problem.

Upon comparison of the experimental values with the theoretical values, one may observe that the measured temperatures were in general slightly higher than those predicted by theory. This was expected and may be attributed to the conduction by the thermocouple sheath material from the hotter test section walls to the sensor tip. It may be very markedly observed from the experimental data that when the solids and fluid temperatures became approximately the same no further changes in temperature occurred along the axis of the test section.

As was anticipated, the void fraction was slightly larger under flow conditions than under static conditions; and, it increased slightly with the flow rates used in this investigation.

Further observations and discussions on some of these factors are contained in the next chapter.

CHAPTER IV

DISCUSSION OF RESULTS

The results of a sieve analysis of the aluminum granules, reported in Appendix D, were utilized in determining the surface area to unit volume ratio. This was done by using the semi-empirical equation

$$S''' = \left(\frac{\alpha_s}{\alpha_v}\right) \sum \frac{w}{d} \tag{4.1}$$

given by DallaValle (32). The portion of the equation inside of the summation was derived from statistical methods, whereas, the constant (α_s/α_v) must be determined by experiment. This constant which depends upon shape, porosity of the individual particles, and packing characteristics was carefully estimated by visual and touch comparison with different sands for which published values are given by DallaValle. (α_s/α_v) was taken as 6.1. This gave a surface area to volume ratio of 2,980 sq. ft./cu. ft. Truly, this unit may then be classified as a compact heat exchanger since a surface area to volume ratio equal to or greater than 200 sq. ft./cu. ft. makes for a compact exchanger (33).

Figure 11 shows pressure distributions for five typical runs selected to show a family of curves with the superficial air mass velocity as parameter. As the superficial air mass velocity increases the pressure differential increases. Of course the static pressure in the lower plenum chamber increases also. By comparing the lower plenum chamber static pressures given in Table 3 with the lowest values shown in Figure 11 the entrance loss may be noted.

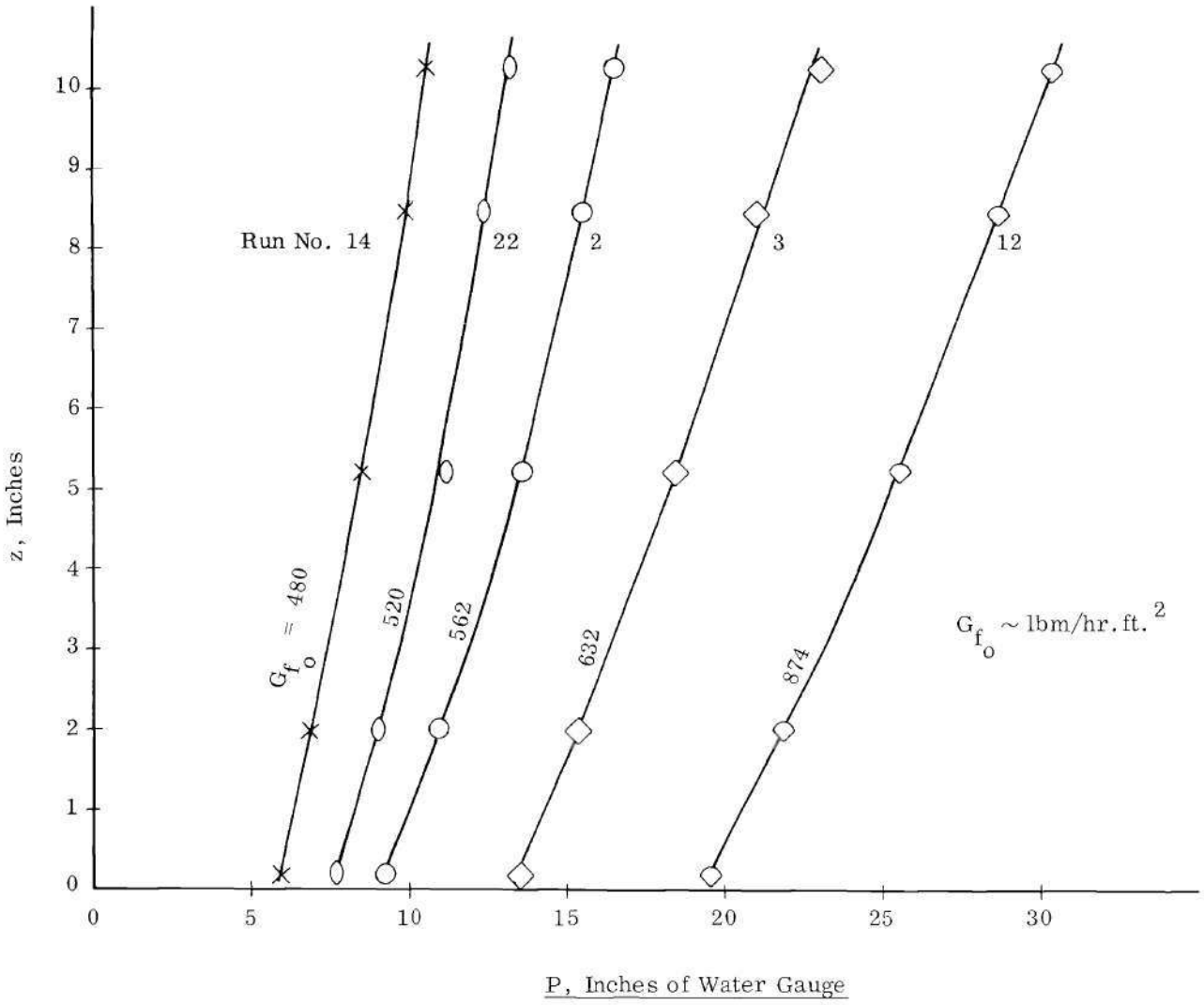

Figure 11. Pressure Distributions

No further consideration of entrance effects was necessary since pressure differentials are the significant factors which must be considered in making application of these findings in a practical system.

The variation of void fraction with superficial air mass velocity is given in Figure 12. For the flow range tested the void fraction increased with the superficial air mass velocity approximately four percent. Special note should be made of the static value of 0.457 determined by using the apparent density given by the manufacturer. This value agrees with the experimental curve when extrapolated to zero mass velocity. Therefore, laminar flow existed throughout the range tested. This linear variation is expected to exist until a transition or turbulent region is reached at which time the void fraction will decrease somewhat due to less drag in turbulent flow.

From these results it is obvious that an error was introduced in the void fraction when the flow of solids and air was stopped in order to measure the temperature distribution of the solids as described in the preceeding chapter. From Figure 12 this maximum error was six percent. However, this does not mean that such an error existed in the overall results. Since the void fraction was so intimately tied up with other parameters, it was only feasible to check its influence on the overall results numerically using the extreme values. Utilizing this variation in void fraction, the overall results were influenced less than one percent when determined by a computer solution of the theoretical equations. (See Appendix E for a Representative Computer Program.)

Including all of the variables which may affect the heat transfer coefficient,

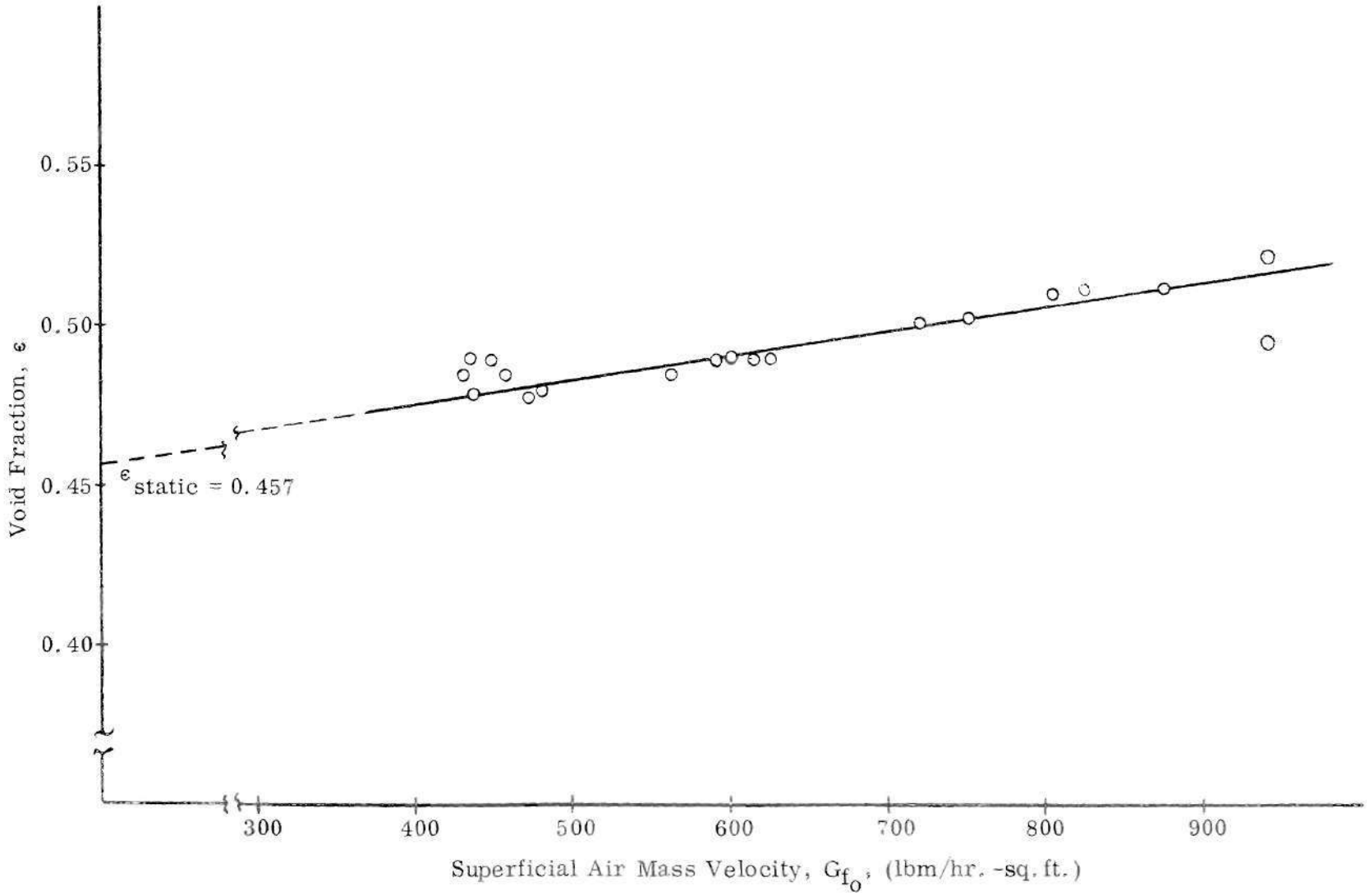

Figure 12. Variation of Void Fraction with Superficial Air Mass Velocity

$$h = \xi\,(G, D_p, \mu_f, k_f, c_{pf}, \epsilon, \Psi, \delta) \qquad (4.2)$$

dimensional analysis yields:

$$\frac{hD_p}{k_f} = \xi_1 \left(\frac{D_p G}{\mu_f}\right)^f \left(\frac{c_{pf}\mu_f}{k_f}\right)^g \times \xi_2(\epsilon, \Psi, \delta) \qquad (4.3)$$

For streamline flow, encountered in this investigation, particle roughness, δ, is an insignificant factor and may be ignored. Assuming spherical particles or using the weight mean diameter, determined from the average sieve diameter, the shape factor, Ψ, may be omitted permitting the function of void fraction to be "absorbed" in the first function of equation (4.3) to give

$$\frac{hD_p}{k_f} = \xi \left(\frac{D_p G}{\mu_f}\right)^f (N_{Pr})^g \qquad (4.4)$$

This form fits the correlation given in Figure 13 when the constants of equation (1.1) are used. It is satisfactory for use under laminar flow conditions, utilizing the weight mean diameter, when properties are evaluated at the mean bulk fluid temperature.

The upper and lower limits respectively for effective thermal conductivity of two component heterogeneous materials as given by Goring and Churchill (27) are:

$$k = k_1\left[1.0 - \epsilon\left(1.0 - \frac{k_2}{k_1}\right)\right] \qquad (4.5)$$

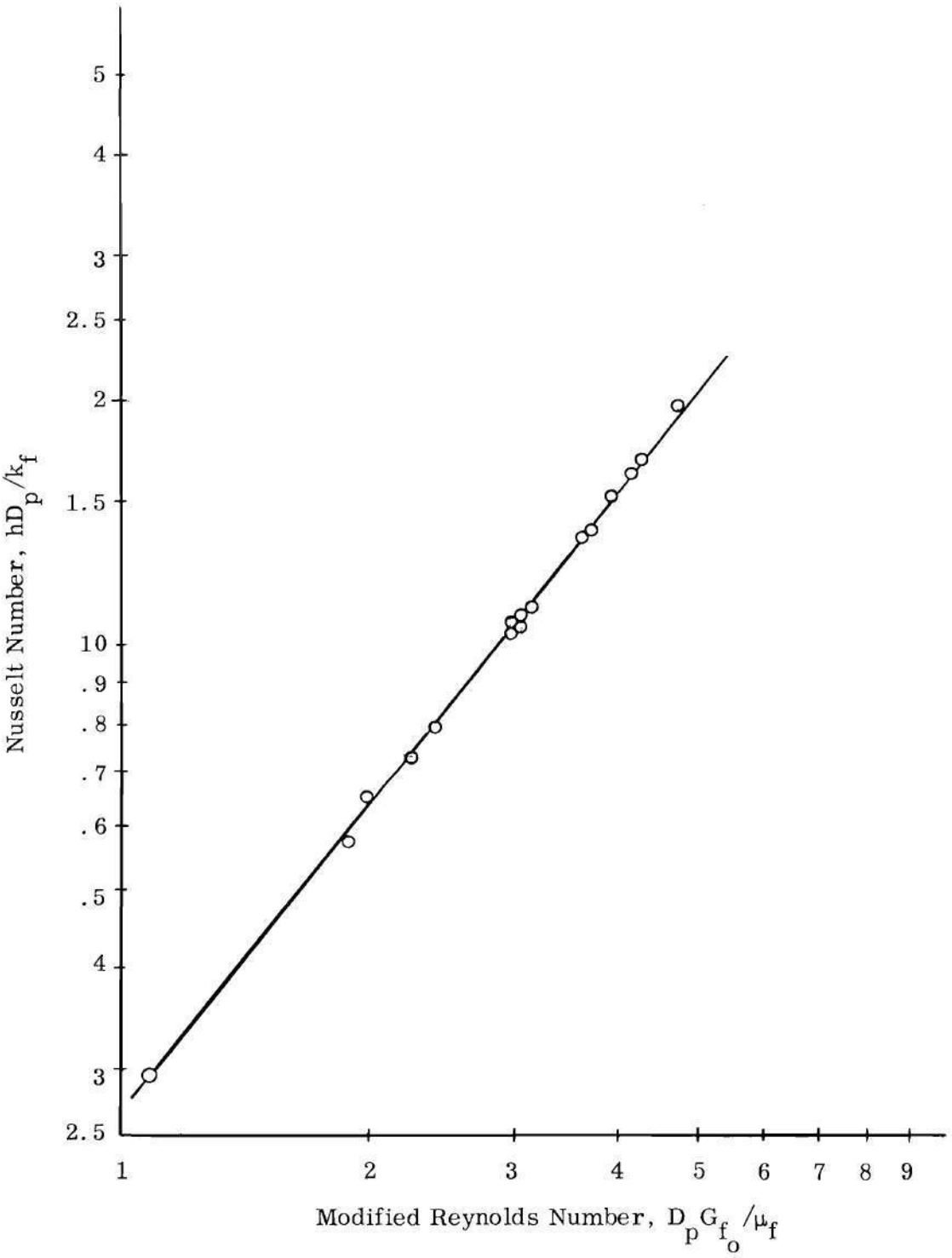

Figure 13. Fluid-to-Particle Heat Transfer Correlation

$$k = \frac{k_1}{1.0 + \varepsilon\left(\frac{k_1}{k_2} - 1.0\right)} \tag{4.6}$$

Using these equations as a guide and the data given by Francl and Kingery (34) and Kunii and Smith (35) careful estimates were made of the effective thermal conductivity of the solids. Since the aluminum granules used in this study may not have the properties desired for a practical system, such a procedure proved adequate for this initial study. The aluminum granules were selected primarily for economic reasons and because the manufacturer published property values for them.

Theoretical temperature distributions are shown in Appendix C along with the experimental values. These theoretical profiles were determined from equations (2.11) and (2.14). Since the effective length had to be determined by trial-and-error, the problem was programed and computed by a Burroughs B-220 Computer. A representative program is given in Appendix E. Due to the nature and size of some of the parameters in the problem at high temperature differentials, the capacity of the B-220 was exceeded. It was then necessary to use the Burroughs B-5500 Computer for higher temperature differentials; e.g., in run number 20 (Figure 19). Large drops in temperature occurred in the entrance region and all of the heat was transferred in a very short length. In general, the measured values of temperature were slightly greater than the theoretical values as discussed in Chapter III. This led to slightly longer effective lengths as measured than predicted by theory. The basic cause was evidently, as stated before, conduction in the sheath material from the hot test section wall to the thermocouple tips. As a result of this the

measured lengths are approximately 20 percent greater than those predicted.

Run numbers 19 through 23 were conducted using the rotary solids feeder which permitted the flow rate of the solids to be greatly reduced. Higher temperature differentials were then possible with low air flow rates.

CHAPTER V

CONCLUSIONS AND RECOMMENDATIONS

The typical graduation range of the aluminum granules furnished by the manufacturer and given in Table 5 agrees extremely well with the measured values of Table 6. The weight mean diameter determined by utilizing the results of Table 6 yielded $D_p = 0.027$ in. The large surface area to volume ratio of 2,980 places such a regenerator in a class of extremely compact heat exchangers. This surface area to volume ratio accounts for only the portion of the bed in which heat transfer actually occurs and does not include the entire bed as some previous investigators have done.

The pressure differential within the moving bed was small as anticipated. Therefore, the system shown in Figure 14 can be utilized as a regenerator with a gas turbine as indicated in Figure 15. For this configuration the length of the connecting tube between the upper and lower chambers would have to be designed for the anticipated pressure differential to prevent excessive leakage. For a more useful system the particles should be constrained to move in a "dense swarm." The void fraction would then be constant for a given material and expressions could be developed for properties such as the effective thermal conductivity. Also, use may be made of such a regenerator in the absence of gravitational fields necessitating constrainment of the particles.

A light-weight material with a high value of thermal diffusivity is desirable for the regenerated media. Further work should be done to optimize a material for this application. Upon establishment of a desirable material careful investigations should be made of thermal and geometric properties.

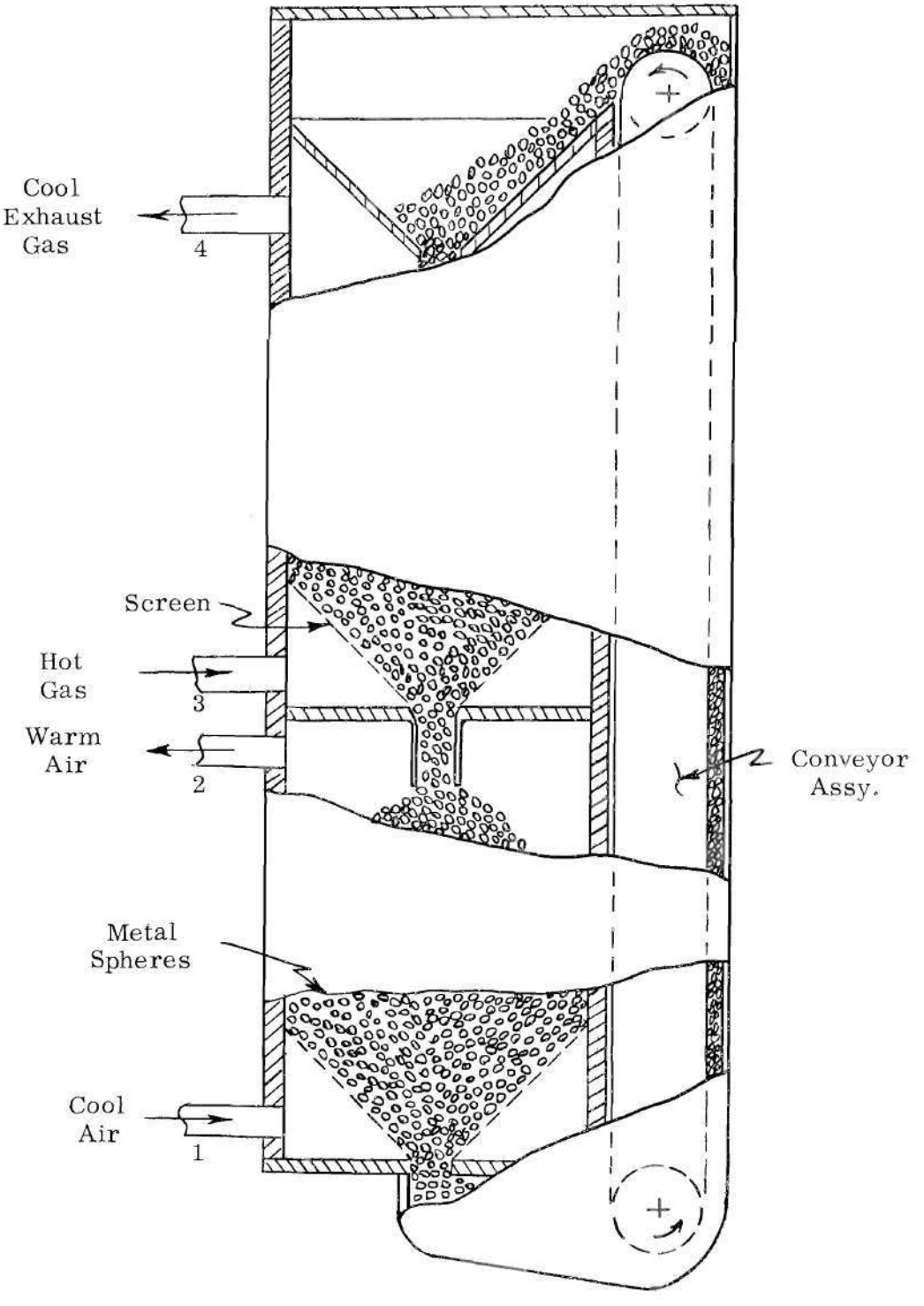

Figure 14. Schematic of Heat Exchanger using the Regenerative Principle

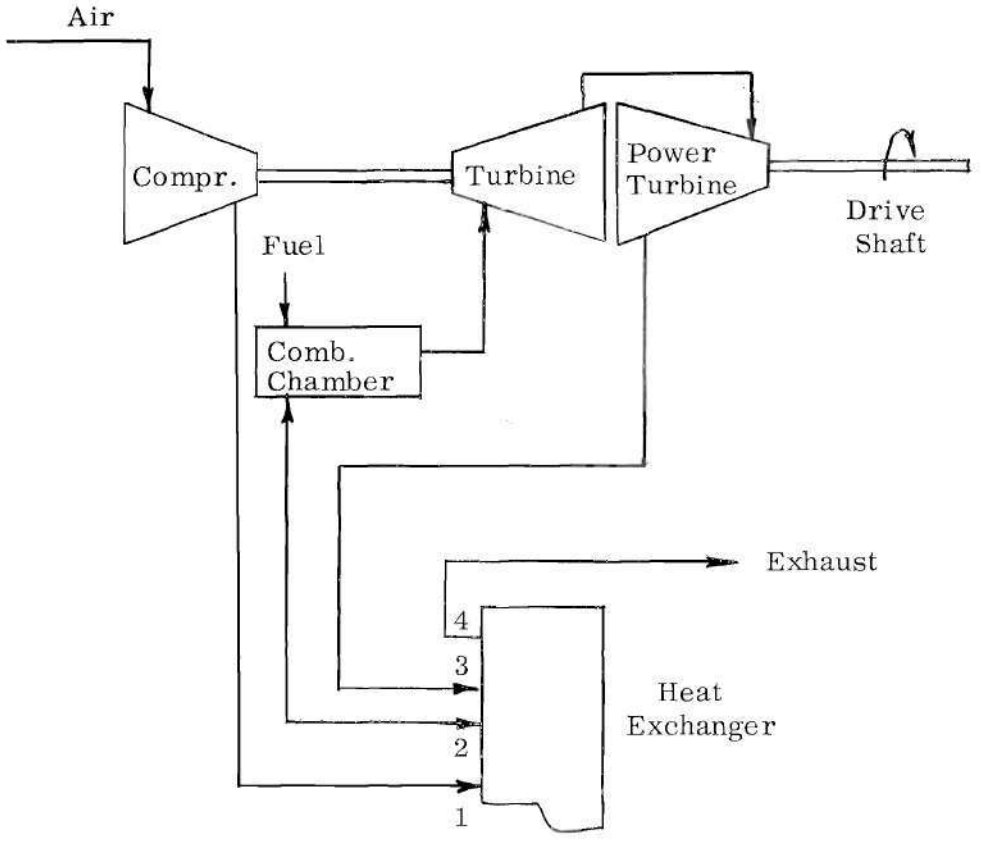

Figure 15. Application to Turbine-powered Mobile Vehicles

A non-abrasive material is desirable.

By making use of the theory of Chapter II the effective length may be predicted whenever properties and flow conditions are known or can be closely estimated. This permits initial design lengths to be established without extensive experimental investigation.

There are at least three methods by which the problem of heat conduction along the thermocouple sheath material may be circumvented. First, with the present experimental apparatus wall temperatures may be measured, the temperature drop along the thermocouple sheath can be calculated, and the temperature profiles may be adjusted accordingly. Secondly, the test section walls may be made of an insulator-type material. Third, suction thermocouples may be installed to periodically sample the flowing fluid. This would have the added advantage of not disturbing the flow of solid particles as much as with the present method. A combination of the second and third methods should reduce the wall heating problem to insignificance.

To extend the work of this investigation a method should be developed to physically constrain the solid particles to move in a "dense swarm". Then with further analytical and experimental work on effective property values a practical model could be built utilizing the principles contained herein.

APPENDIX A

DERIVATION OF EQUATIONS

For the analysis replace the actual system by an idealized model, containing uniformly dispersed parallel cylindrical passages, which will produce the same momentum and heat transfer effects. It should be noted that no size or cross-sectional shape limitations have been made on the cylindrical passages, since this will depend upon momentum and heat transfer conditions. The volume of the "capillary tubes" will be taken equal to the void volume of the actual system. The fluid, of thermal conductivity k_f, flows through these "capillary tubes." The "solid" portion of the model has an effective thermal conductivity $k_{s,e}$ which will be used to account for the drop across the film resistance between the particles. Therefore, one may anticipate that $k_{s,e} < k_s$.

Defining the void fraction or porosity ϵ as the ratio of void volume to total volume, the flow area per unit total area for the fluid is $A_f = \epsilon$. Therefore, the solid area is $A_s = (1 - \epsilon)$ per unit total area.

Consider a vertical cylindrical duct of constant cross-section as shown in Figure 16.

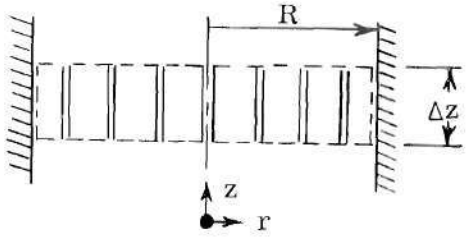

Figure 16. Control Volume for Analysis

Consider a control volume of length Δz and radius R. Base the fluid velocity on that which would exist if the fluid occupied the duct alone. This velocity will be referred to as the "superficial fluid velocity." For adiabatic walls, which will be assumed, and the previously described flow conditions the temperature distribution will essentially be one-dimensional for both the fluid and solids. Since there are two unknowns, T_s and T_f, there must be two differential equations describing the system. One equation will be obtained by making a heat balance on all of the material, solid and fluid, in a differential volume. The second equation will be derived from a heat balance on the solids alone.

Taking Δz much larger than the particle size, for an element balance, under steady state conditions for the solid and fluid we get:

$$\underbrace{(1-\epsilon)\left[\pi R^2 q_s''\Big|_{z+\Delta z} - \pi R^2 q_s''\Big|_z\right]}_{\text{Thermal energy conducted by solids}} + \underbrace{\epsilon\left[\pi R^2 q_f''\Big|_{z+\Delta z} - \pi R^2 q_f''\Big|_z\right]}_{\text{Thermal energy conducted by fluid}}$$

$$+ \underbrace{(1-\epsilon)\left[\pi R^2 G_s h_s\Big|_{z+\Delta z} - \pi R^2 G_s h_s\Big|_z\right]}_{\text{Enthalpy transfer of solids}} + \underbrace{\left[\pi R^2 G_{f_o} h_f\Big|_{z+\Delta z} - \pi R^2 G_{f_o} h_f\Big|_z\right]}_{\text{Enthalpy transfer of fluid}} = 0 \qquad (A.1)$$

The above equation results from the application of the First Law of Thermodynamics where shear work, kinetic and potential energy changes, and dissipative effects have been neglected due to negligible wall effects for $d_t/d_p \gtrsim 10$, low velocities, small elevation changes, and small velocity gradients, respectively. G_s and G_{f_o} will have the same signs for cocurrent flow and opposite for countercurrent flow.

Now

$$G_s = \rho_s V_s = \text{Constant} \tag{A.2}$$

$$G_{f_o} = \rho_f V_{f_o} = \text{Constant} \tag{A.3}$$

$$h_f = c_{pf} T_f \text{ for an ideal gas} \tag{A.4}$$

Therefore, using equations (A.2), (A.3), and (A.4) and dividing by $\pi R^2 \Delta z$, equation (A.1) becomes:

$$(1-\epsilon)\left[\frac{q_s''\big|_{z+\Delta z} - q_s''\big|_z}{\Delta z}\right] + \epsilon\left[\frac{q_f''\big|_{z+\Delta z} - q_f''\big|_z}{\Delta z}\right]$$

$$+ (1-\epsilon)\left[\frac{\rho_s V_s h_s\big|_{z+\Delta z} - \rho_s V_s h_s\big|_z}{\Delta z}\right]$$

$$+\left[\frac{\rho_f V_{f_o} c_{pf} T_f\big|_{z+\Delta z} - \rho_f V_{f_o} c_{pf} T_f\big|_z}{\Delta z}\right] = 0 \tag{A.5}$$

We may now take the limit as $\Delta z \to 0$ if it is agreed that the resulting equation gives average values rather than point values, since the system is not a continuum in the strictest sense.

$$(1-\epsilon)\frac{\partial q_s''}{\partial z} + \epsilon\frac{\partial q_f''}{\partial z} + (1-\epsilon)\rho_s V_s \frac{\partial h_s}{\partial z} + \rho_f V_{f_o} c_{pf} \frac{\partial T_f}{\partial z} = 0 \tag{A.6}$$

Using Fourier's law of heat conduction,

$$q_s'' = -k_{s,e} \frac{\partial T_s}{\partial z} \tag{A.7}$$

$$q_f'' = -k_f \frac{\partial T_f}{\partial z} \tag{A.8}$$

Substituting equations (A.7) and (A.8) into equation (A.6),

$$(1-\epsilon)\frac{\partial}{\partial z}\left(-k_{s,e}\frac{\partial T_s}{\partial z}\right) + \epsilon\frac{\partial}{\partial z}\left(-k_f\frac{\partial T_f}{\partial z}\right) + (1-\epsilon)\rho_s V_s \frac{\partial h_s}{\partial z}$$

$$+ \rho_f V_{f_o} c_{pf} \frac{\partial T_f}{\partial z} = 0 \tag{A.9}$$

Considering the solid alone, the heat balance for steady state gives:

$$\underbrace{(1-\epsilon)\left[\pi R^2 q_s''\Big|_{z+\Delta z} - \pi R^2 q_s''\Big|_z\right]}_{\text{Thermal energy conducted}} + \underbrace{(1-\epsilon)\left[\pi R^2 G_s h_s\Big|_{z+\Delta z} - \pi R^2 G_s h_s\Big|_z\right]}_{\text{Enthalpy transfer of solids}}$$

$$\underbrace{-hS(T_f - T_s)}_{\text{Heat convected from fluid to solid}} = 0 \tag{A.10}$$

where S is the effective surface area of the particles in the length Δz and h is the local convective heat transfer coefficient. Dividing equation (A.10) by $\pi R^2 \Delta z$,

$$(1 - \varepsilon)\left[\frac{q_s''\big|_{z+\Delta z} - q_s''\big|_z}{\Delta z}\right] + (1 - \varepsilon)\left[\frac{G_s h_s\big|_{z+\Delta z} - G_s h_s\big|_z}{\Delta z}\right]$$

$$- \left[\frac{hS\,(T_f - T_s)}{\pi R^2 \Delta z}\right] = 0 \qquad \text{(A.11)}$$

Noting that $\pi R^2 \Delta z = \Delta \underline{V}$ we may let $S/\Delta \underline{V} \equiv S'''$. Therefore, taking the limit as $\Delta z \to 0$ and using Fourier's law of heat conduction, we get:

$$(1 - \varepsilon)\frac{\partial}{\partial z}\left(-k_{s,e}\frac{\partial T_s}{\partial z}\right) + (1 - \varepsilon)\rho_s V_s \frac{\partial h_s}{\partial z} - hS'''(T_f - T_s) = 0 \qquad \text{(A.12)}$$

which is at the same stage of development as equation (A.6).

In order to simplify equations (A.6) and (A.12) recall that for any pure substance an equation of state may be written (at least functionally) in terms of three thermodynamic properties. Hence, an expression for enthalpy may be written as a function of temperature and specific volume, i.e.,

$$h = h(T, v)$$

From the chain rule for partial differentiation,

$$\frac{dh}{dT} = \frac{\partial h}{\partial T}\Big)_v + \frac{\partial h}{\partial v}\Big)_T \frac{dv}{dT}$$

Considering the substance to pass through a constant pressure process,

$$\frac{\partial h}{\partial T}\Big)_p = \frac{\partial h}{\partial T}\Big)_v + \frac{\partial h}{\partial v}\Big)_T \frac{\partial v}{\partial T}\Big)_p$$

But for a solid

$$\frac{\partial v}{\partial T}\Big)_p \cong 0$$

Therefore

$$\frac{\partial h}{\partial T}\Big)_p \cong \frac{\partial h}{\partial T}\Big)_v$$

Also,

$$\frac{dh}{dz} = \frac{\partial h}{\partial T}\Big)_v \frac{dT}{dz} + \frac{\partial h}{\partial v}\Big)_T \frac{dv}{dz}$$

and $dv/dz = 0$ for a solid.

Therefore,

$$\frac{\partial h_s}{\partial z} = \frac{\partial h}{\partial T}\Big)_p \frac{\partial T_s}{\partial z}$$

But, by definition

$$c_p \equiv \frac{\partial h}{\partial T}\Big)_p$$

and for a solid $c_p = c$. Hence,

$$\frac{\partial h_s}{\partial z} = c_s \frac{\partial T_s}{\partial z} \tag{A.13}$$

Using this along with the assumption that $k_{s,e}$ is constant for a given set of flow conditions and that k_f may be replaced by its mean-value $\bar{k}_f$ defined by

$$k_f \equiv \frac{\int_a^z k_f \, dT}{T_{f_z} - T_{f_a}}$$

equations (A. 6) and (A. 12) simplify to give respectively

$$-(1 - \varepsilon) k_{s,e} \frac{d^2 T_s}{dz^2} - \varepsilon \bar{k}_f \frac{d^2 T_f}{dz^2} + (1 - \varepsilon) G_s c_s \frac{dT_s}{dz} + G_{f_o} c_{pf} \frac{dT_f}{dz} = 0$$

$$-(1-\epsilon)\,k_{s,e}\,\frac{d^2T_s}{dz^2}+(1-\epsilon)\,G_s c_s\,\frac{dT_s}{dz}-hS'''(T_f-T_s)=0$$

Dividing both equations by $-(1-\epsilon)\,k_{s,e}$,

$$\frac{d^2T_s}{dz^2}+\frac{\epsilon\,\bar{k}_f}{(1-\epsilon)\,k_{s,e}}\,\frac{d^2T_f}{dz^2}-\frac{G_s c_s}{k_{s,e}}\,\frac{dT_s}{dz}-\frac{G_{f_o} c_{pf}}{(1-\epsilon)k_{s,e}}\,\frac{dT_f}{dz}=0 \qquad \text{(A.14)}$$

$$\frac{d^2T_s}{dz^2}-\frac{G_s c_s}{k_{s,e}}\,\frac{dT_s}{dz}+\frac{hS'''}{(1-\epsilon)k_{s,e}}\,(T_f-T_s)=0 \qquad \text{(A.15)}$$

APPENDIX B

ANALYSIS OF THE ROOTS OF THE SOLUTION EQUATIONS

The equivalent algebraic expression for the cubic portion of equation (2.7b)

$$m^3 + pm^2 + qm + r = 0 \tag{B.1}$$

where

$$p \equiv \beta + \frac{\eta}{\alpha}$$

$$q \equiv (-)\left[\frac{\lambda(\alpha + 1) - \beta\eta}{\alpha}\right]$$

$$r \equiv (-)\left[\frac{\lambda(\beta + \eta)}{\alpha}\right]$$

may be solved by the cubic equation. Before preceeding it is necessary to investigate the term $(b^2/4 + a^3/27)$ where

$$a \equiv q - \frac{p^2}{3}$$

$$b \equiv \frac{2}{27} p^3 - \frac{pq}{3} + r$$

since this will determine the nature of the roots and hence the form of the solution of the differential equations.

$$a^3 = q^3 - p^2 q^2 + \frac{p^4 q}{3} - \frac{p^6}{27}$$

$$b^2 = \frac{4}{(27)^2} p^6 - \frac{4}{81} p^4 q + \frac{4}{27} p^3 r + \frac{p^2 q^2}{9} - \frac{2pqr}{3} + r^2$$

Therefore,

$$\left(\frac{b^2}{4} + \frac{a^3}{27}\right) = \frac{p^3 r}{27} - \frac{p^2 q^2}{108} - \frac{pqr}{6} + \frac{r^2}{4} + \frac{q^3}{27} \qquad \text{(B. 2)}$$

Going back to the definitions of the various parameters it can be seen that the first and last terms of equation (B. 2) are negative with the remaining terms being positive. Considering algebraic signs also the fourth term is the only positive one, and the question arises

$$\left|\frac{p^3 r}{27} + \frac{p^2 q^2}{108} + \frac{pqr}{6} + \frac{q^3}{27}\right| \overset{?}{>} \frac{r^2}{4} \qquad \text{(B. 3)}$$

Considering only the term pqr/6,

$$p \equiv \beta + \frac{\pi}{\alpha} > \frac{\pi}{\alpha}$$

$$q \equiv (-)\left[\frac{\lambda(\alpha+1)-\beta\eta}{\alpha}\right] > (-)\lambda\left(\frac{1}{\alpha}+1\right)$$

$$r \equiv (-)\ \frac{\lambda(\beta+\eta)}{\alpha}$$

neglecting β,

$$r > (-)\ \frac{\eta\lambda}{\alpha}$$

Hence,

$$\frac{pqr}{6} > \frac{1}{6}\left(-\frac{r^2}{\lambda}\right)\left[-\lambda\left(\frac{1}{\alpha}+1\right)\right] >^{?} \frac{r^2}{4}$$

$$\frac{1}{\alpha} + 1 > \frac{3}{2}$$

$$\alpha < 2$$

But α is always less than unity; hence, the inequality of equation (B. 3) is true. Therefore, $(b^2/4 + a^3/27) < 0$ and there are three real and unequal roots of equation (2. 7b). The roots are given by:

$$m_1 = 2\sqrt{-\frac{a}{3}}\ \cos\ \frac{\varphi}{3} - \frac{p}{3} \qquad \text{(B. 4)}$$

$$m_2 = 2 \sqrt{-\frac{a}{3}} \cos\left(\frac{\varphi}{3} + \frac{2\pi}{3}\right) - \frac{p}{3} \qquad \text{(B. 5)}$$

$$m_3 = 2 \sqrt{-\frac{a}{3}} \cos\left(\frac{\varphi}{3} + \frac{4\pi}{3}\right) - \frac{p}{3} \qquad \text{(B. 6)}$$

where

$$\varphi = \arccos\left(-\frac{b}{2} \div \sqrt{-\frac{a^3}{27}}\right) \qquad \text{(B. 7)}$$

APPENDIX C

EXPERIMENTAL AND THEORETICAL DATA

The experimental and theoretical data obtained in the course of this investigation are given on the subsequent pages. Figures 17, 18, and 19 show some typical theoretical and experimental temperature distributions. Typical experimental profiles for other runs are given in Figures 20 and 21. Tables 1, 2, 3, and 4 summarize all of the experimental data taken.

Properties utilized in the determination of these values are given in Appendix D.

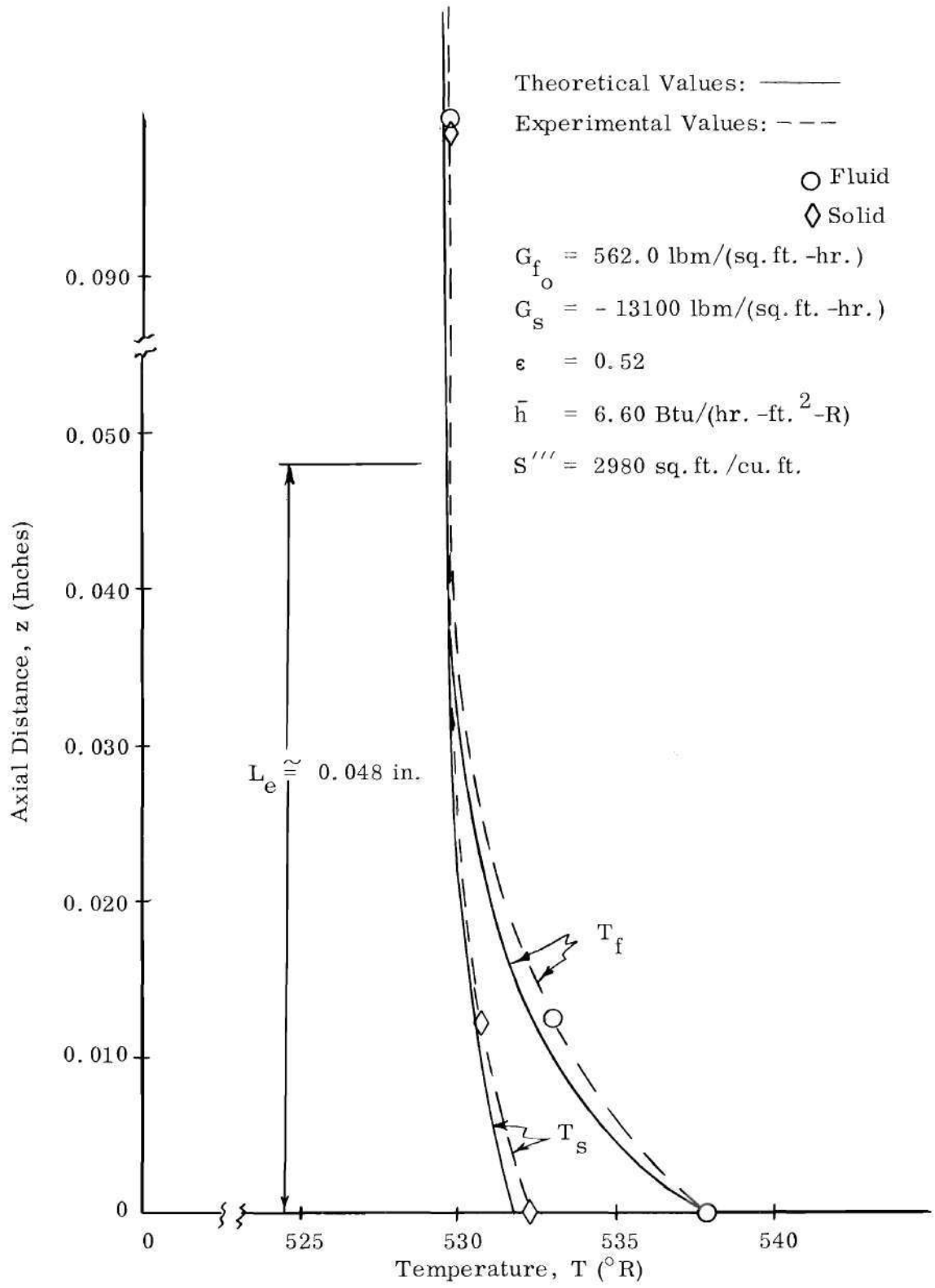

Figure 17. Temperature Distribution ~ Run No. 2

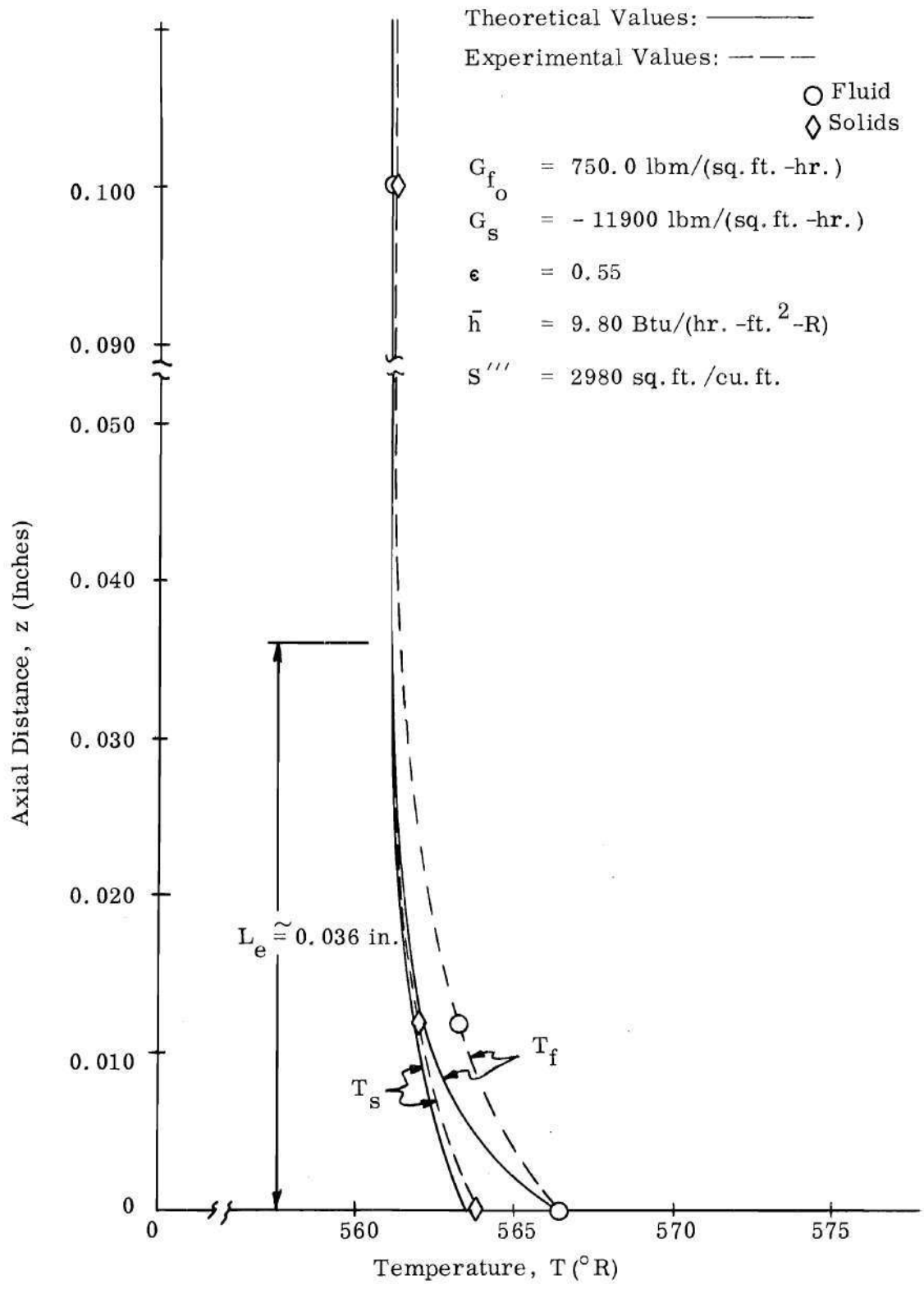

Figure 18. Temperature Distribution ~ Run No. 16

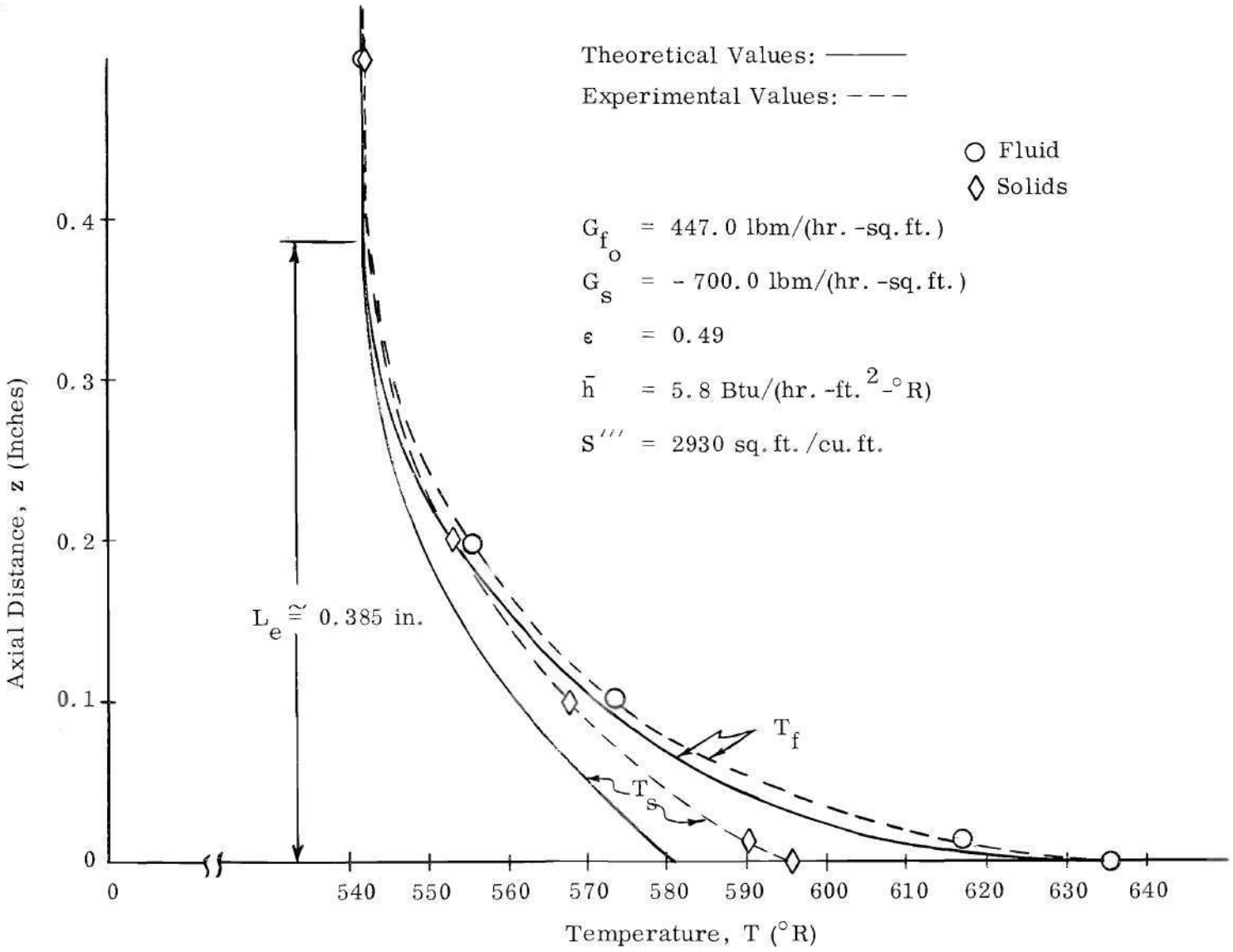

Figure 19. Temperature Distribution ~ Run No. 20

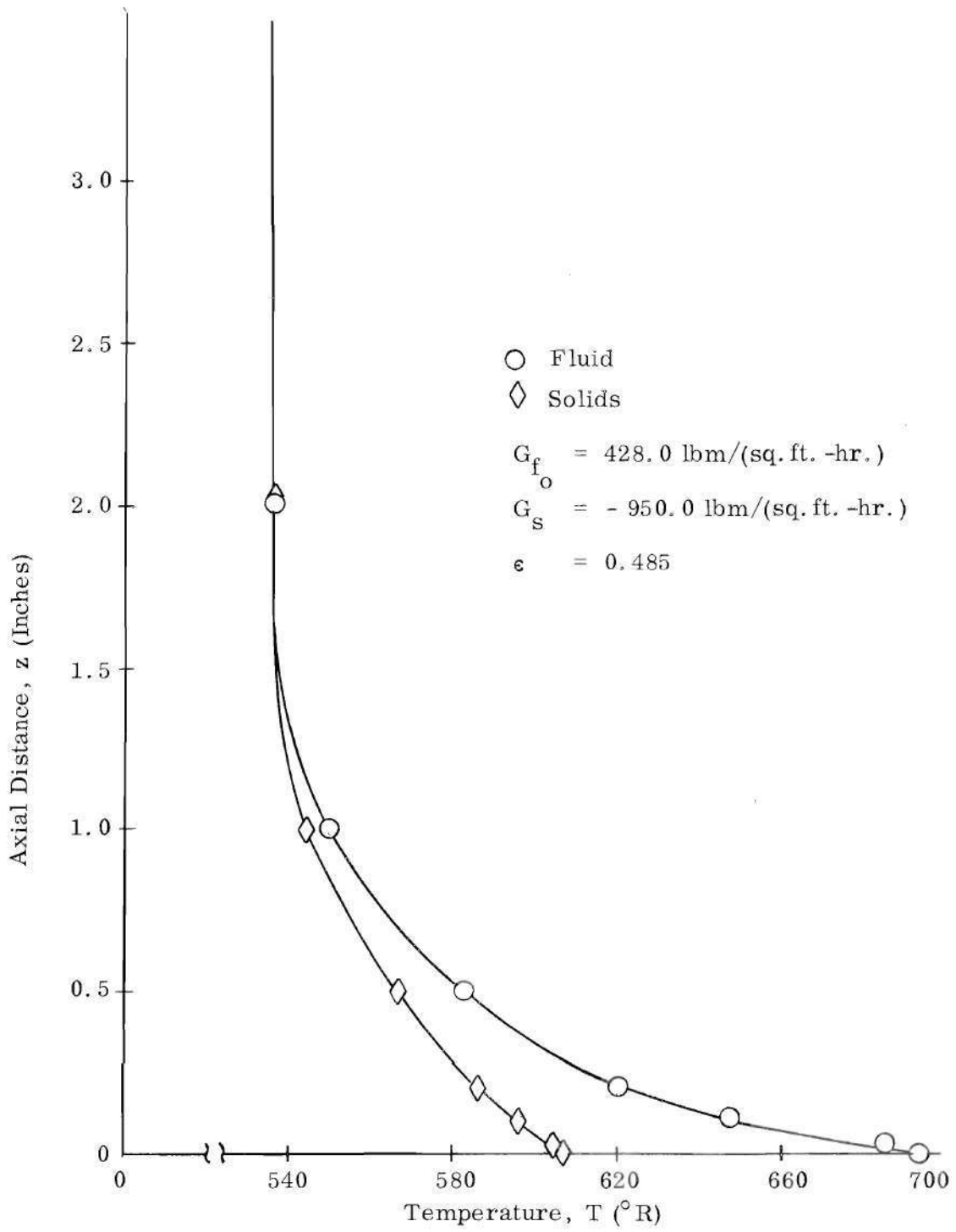

Figure 20. Experimental Temperature Distribution ~ Run No. 21

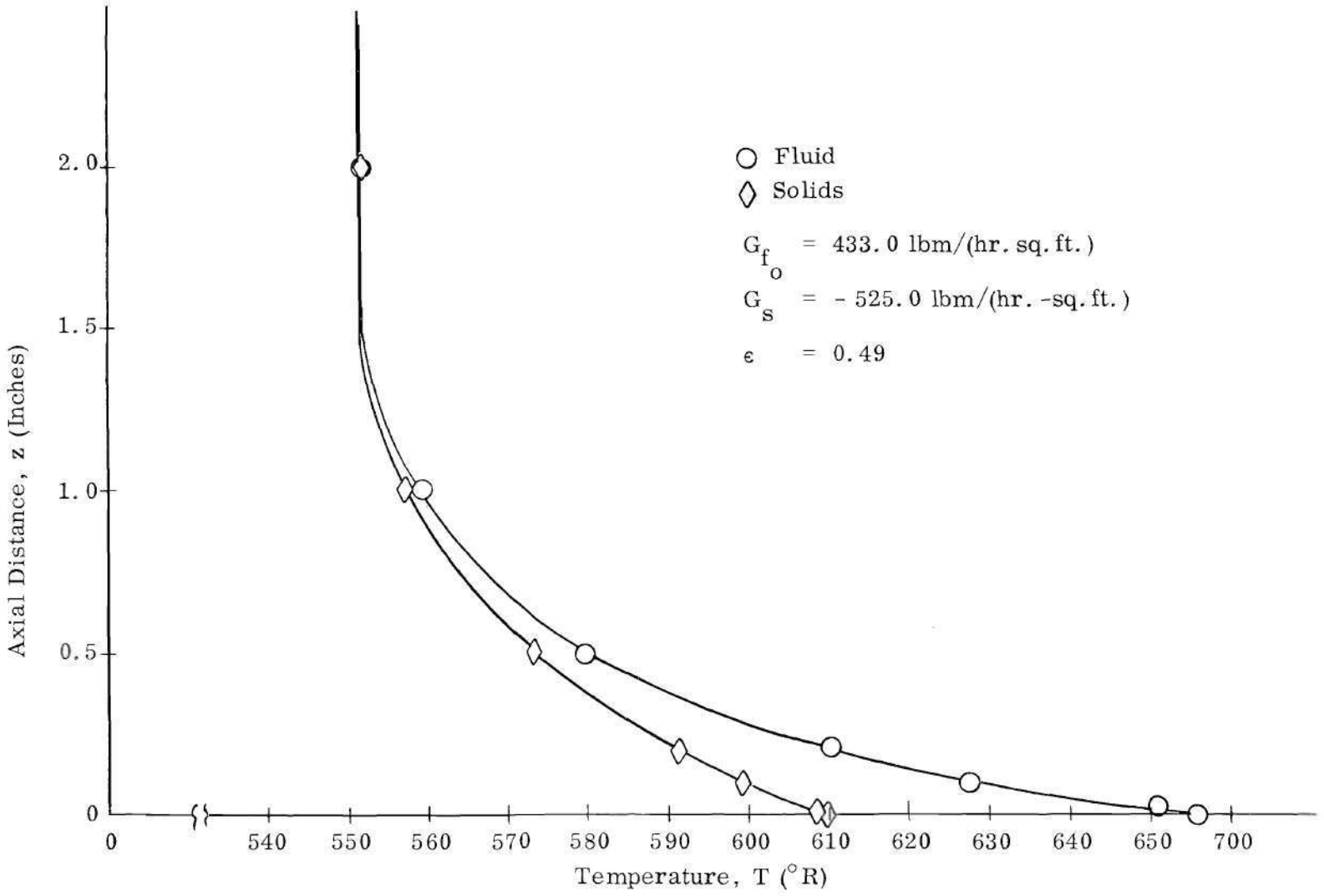

Figure 21. Experimental Temperature Distribution ~ Run No. 23

Table 1. Experimental Data

Run No.	Solids Flow Rate, G_s (lbm/hr.-sq.ft.)	Air Flow Rate, Gf_o (lbm/hr.-sq.ft.)	Void Fraction, ε	Heater Voltage
1	-15,400	940	0.52	43
2	-14,100	562	0.485	40
3	-12,900	625	0.49	40
4	-11,900	600	0.492	40
5	-11,900	600	0.49	50
6	-13,200	592	0.489	50
7	-10,000	615	0.491	45
8	-12,200	625	0.491	55
9	-18,900	828	0.512	45
10	-13,000	825	0.513	45
11	-16,600	805	0.51	45
12	-15,200	874	0.514	55
13	-10,000	720	0.502	40
14	- 7,240	480	0.48	50
15	- 7,040	480	0.48	55
16	-11,900	750	0.503	50
17	- 6,420	475	0.48	55
18	-10,900	470	0.478	70
19	- 472	434	0.47	60
20	- 700	447	0.49	70
21	- 950	428	0.485	75
22	- 800	520	0.485	75
23	- 525	433	0.49	70

Table 2. Measured Differential Pressures*

Run No.	p_1	p_2	p_3	p_4	p_5
1	0.76	2.08	4.95	6.70	7.20
2	0.46	2.05	4.70	6.60	7.60
3	0.53	2.25	5.30	8.00	10.00
4	0.54	2.26	5.32	7.80	9.20
5	0.55	2.25	5.20	7.80	9.00
6	0.56	2.18	5.16	7.60	8.85
7	0.56	1.66	3.70	5.40	6.40
8	0.61	1.78	3.90	5.60	6.60
9	0.78	2.39	5.42	9.80	11.80
10	0.82	2.40	5.45	9.90	11.80
11	0.82	2.28	5.37	9.40	11.40
12	0.93	3.18	6.80	10.00	11.80
13	0.66	2.42	5.80	8.80	10.60
14	0.38	1.33	2.95	4.40	5.00
15	0.48	1.45	3.15	4.40	5.40
16	0.70	2.08	5.50	7.60	9.30
17	0.40	1.40	3.05	4.20	5.40
18	0.39	1.63	3.60	5.20	6.10
19	0.69	2.12	5.30	7.40	8.60
20	0.65	2.05	5.30	7.20	8.40
21	0.77	2.18	5.25	8.40	9.60
22	0.50	1.85	4.00	5.20	6.00
23	0.68	2.03	5.00	6.40	7.20

* inches water gauge

Table 3. Measured Pressures

Run No.	Barometric, p_o (in. Hg)	Lower Plenum Chamber, p_{static} (inches water gauge)
1	29.20	15.00
2	29.20	8.80
3	29.24	13.00
4	29.24	13.40
5	29.24	12.60
6	29.24	13.00
7	29.30	9.60
8	29.30	9.80
9	29.38	14.40
10	29.38	16.20
11	29.38	17.00
12	29.38	18.60
13	29.03	11.80
14	29.30	5.60
15	29.30	5.80
16	29.18	9.80
17	28.95	6.05
18	29.34	11.40
19	29.48	10.00
20	29.16	9.60
21	29.14	11.80
22	29.14	7.20
23	28.71	9.40

Table 4. Measured Temperatures

Run No.	T_1, °F		T_2, °F		T_3, °F		T_4, °F	
	Air	Solids	Air	Solids	Air	Solids	Air	Solids
1	87.8	84.1	74.8	75.0	75.4		75.4	75.7
2	77.9	72.0	70.9	69.9	71.2		69.6	69.6
3	93.2		91.5		91.5		91.5	
4	93.5	92.8	91.5	91.5	92.0	91.8	91.5	
5	96.0	94.0	92.5	92.2	92.9		92.4	92.0
6	86.1	85.0	81.4	81.0	82.1		81.4	81.1
7	84.7	83.0	81.5	79.1			81.5	79.0
8	100.0	96.5	97.8	96.0			96.0	95.9
9	84.2	81.5	79.2	79.4			79.2	79.4
10	96.4	95.5	92.2	92.1			92.1	92.0
11	102.4	100.5	98.5	98.7			98.5	98.5
12	103.8	101.4	99.0	98.9			98.9	98.8
13	93.3	87.5	84.4	84.3			83.1	83.0
14	97.6	93.4	95.2	96.0			94.8	94.9
15	94.1	93.0	88.8	89.6			88.6	88.6
16	106.3	103.8	102.1	101.8			101.3	101.2
17	110.5		105.8				105.7	
18	117.5	116.6	96.2	96.2			96.2	96.2
19	211.2	201.3	185.4	185.2			183.7	182.4
20	175.4	168.2	151.8	147.7			82.3	82.3
21	236.1	146.8	187.8	136.2			161.1	126.0
22	200.0	194.0	185.6	182.3			184.6	181.6
23	215.0	150.0	167.5	138.9			150.0	131.2

Table 4. Measured Temperatures (Continued)

Run No.	T_5, °F		T_6, °F		T_7, °F		T_8, °F	
	Air	Solids	Air	Solids	Air	Solids	Air	Solids
1	74.7	74.7	74.7	74.7	74.7	74.7	74.7	74.7
2	69.6	69.6	69.6	69.6	69.6	69.6	69.6	69.6
3	91.5		91.5		91.5		91.5	
4	91.5		91.5		91.5			
5	92.4	92.0	92.4	92.0	92.4	92.0	92.4	92.0
6	81.4	81.1	81.4	81.4	81.4	81.4	81.4	81.4
7	81.5	79.0	81.5	79.0	81.5	79.0	81.5	79.0
8	96.0	95.9	96.0	95.9	96.0	95.9	96.0	95.9
9	79.2	79.4	79.2	79.4	79.2	79.4	79.2	79.4
10	92.1	92.0	92.1	92.0	92.1	92.0	92.1	92.0
11	98.5	98.5	98.5	98.5	98.5	98.5	98.5	98.5
12	98.9	98.8	98.9	98.8	98.9	98.8	98.9	98.8
13	80.1	80.0	80.1	80.0	80.1	80.0	80.1	80.0
14	94.8	94.8	94.8	94.8	94.8	94.8	94.8	94.8
15	88.6	88.6	88.6	88.6	88.6	88.6	88.6	88.6
16	101.3	101.2	101.3	101.2	101.3	101.2	101.3	101.2
17	105.7		105.7					
18	96.2	96.2	96.2	96.2	96.2	96.2	96.2	96.2
19	172.6	171.0	157.5	157.0	141.3	141.0	87.5	87.5
20	82.3	82.2	82.3	82.2	82.3	82.2	82.3	82.2
21	123.2	106.9	90.0	84.2	76.3	76.3	76.3	76.3
22	173.2	170.4	161.5	157.6	145.4	143.0	97.7	96.5
23	118.9	113.2	98.8	97.2	91.5	91.5	91.5	91.5

Table 4. Measured Temperatures (Continued)

Run No.	T_9, °F		T_{10}, °F		T_{11}, °F		T_{12}, °F	
	Air	Solids	Air	Solids	Air	Solids	Air	Solids
1	74.7	74.7	80.3		80.6		80.0	
2	69.6	69.6	69.6	69.6	69.6	69.6	69.6	
3	91.5		91.5					
4							91.5	
5	92.4	92.0	92.4		92.4		92.4	
6	81.4	81.1	81.4	81.1	81.4	81.1	81.4	81.1
7	81.5	79.0	81.5	79.0	81.5	79.0	81.5	79.0
8	96.0	95.9	96.0	95.9	96.0	95.9	96.0	95.9
9	79.2	79.4	79.2	79.4	79.2	79.4	79.2	79.4
10	92.1	92.0	92.1	92.0	92.1	92.0	92.1	92.0
11	98.5	98.5	98.5	98.5	98.5	98.5	98.5	98.5
12	98.9	98.8	98.9	98.8	98.9	98.8	98.9	98.8
13	80.1	80.0	80.1	80.0	80.1	80.0	80.1	80.0
14	94.8	94.8	94.8	94.8	94.8	94.8	94.8	94.8
15	88.6	88.6	88.6	88.6	88.6	88.6	88.6	88.6
16	101.3	101.2	101.3		101.3		101.3	
17			105.7					
18	96.2	96.2	96.2	96.2	96.2	96.2	96.2	96.2
19	87.5	87.5	87.5	87.5	87.5	87.5	87.5	87.5
20	82.3	82.2	82.3	82.2	82.3	82.2	82.3	82.3
21	76.3	76.3	76.3	76.3	76.3	76.3	76.3	76.3
22	96.5	96.5	96.5	96.5	96.5	96.5	96.5	96.5
23	91.5	91.5	91.5	91.5	91.5	91.5	91.5	91.5

Table 4. Measured Temperatures (Continued)

Run No.	T_{13}, °F		T_{14}, °F		T_{15}, °F		T_{16}, °F	
	Air	Solids	Air	Solids	Air	Solids	Air	Solids
1	86.1		85.6		75.2		212.1	
2	69.6				59.5		197.0	
3			91.5		59.3		201.3	
4	91.5		91.5					
5	92.4	92.0	92.4	92.0	78.2		223.5	
6	81.4	81.1	81.4		67.8		234.6	238.8
7	81.5	79.0	81.5	79.0	66.7	66.7	240.2	245.2
8	96.0	95.9	96.0	95.9	75.0	76.2	288.1	279.1
9	79.2	79.4	79.2	79.4			267.4	274.0
10	92.1	92.0	92.1	92.0	63.2		244.6	
11	98.5	98.5	98.5	98.5	72.8	72.8	242.1	232.5
12	98.9	98.8	98.9	98.8			334.6	297.8
13	80.1	80.0	80.1	80.0			257.0	220.7
14	94.8	94.8	94.8	94.8	66.0	67.5	285.7	267.5
15	88.6	88.6	88.6	88.6			337.3	314.1
16	101.3		101.3	101.2	70.0	70.5	275.6	269.6
17								
18	96.2	96.2	96.2	96.2	63.1	63.2	356.5	365.4
19	87.5	87.5	87.5	87.5	298.5	349.5	425.1	423.2
20	82.3	82.2	82.2	82.2	239.2	295.2	302.6	473.0
21	76.3	76.3	76.3	76.3	289.0	276.2	548.0	545.5
22	96.5	96.5	96.5	96.5	303.6	306.7	541.5	539.2
23	91.5	91.5	91.5	91.5	360.2	382.2	541.5	533.0

Table 4. Measured Temperatures (Continued)

Run No.	T_{17}, °F		T_{18}, °F		T_0, °F
	Air	Solids	Air	Solids	Ambient
1	83.7		80.6		77.0
2	72.7		73.4	70.6	77.0
3	77.0		92.0		77.0
4			91.5		75.0
5	79.6		92.4	92.0	75.0
6	79.5		81.5	81.4	78.0
7	74.2	74.6	84.4	80.7	78.0
8	70.2	69.0	99.7	96.1	78.0
9	73.1	72.1	83.0	80.7	78.2
10	73.5		95.1		78.2
11	68.4	68.1	99.8	98.5	78.2
12	70.5	70.5	101.2	100.5	81.0
13	77.1	77.1	87.6	87.1	82.0
14	75.4	74.3	96.4	96.0	80.8
15	75.8	76.3	92.6	91.6	81.0
16	76.4	76.1	103.2	102.2	83.5
17			110.0		79.0
18	76.7	76.3	106.1	103.7	82.3
19	71.2	72.7	191.2	187.0	78.0
20	76.5	76.9	156.7	152.5	80.2
21	76.3	76.7	226.0	144.8	85.5
22	73.5	73.6	191.2	188.6	87.0
23	69.8	70.5	190.6	148.5	78.0

APPENDIX D

PROPERTIES

Table 5. Typical Graduation Range of Aluminum Granules*

Mesh	Weight Percentage Range
16	0-5
-16 18	0-5
-18 20	2-10
-20 30	65-85
-30 40	15-25
-40	0-5

Table 6. Actual Measured Values of Aluminum Granules

Mesh	Weight Percentage	Mean Sieve diameter (in.)
20	10.1	0.0470
-20 30	67.0	0.0272
-30 40	22.5	0.0176
-40	0.4	0.0130

* Average Density: 92.0 lbm/cu. ft.

* Specific Heat: 0.21 Btu/lbm-R

* Aluminum EXXO 16-40 Sphere
Aluminum Metallurgical Granules
P. O. Box 6232
Kansas City 26, Missouri

Static Void Fraction, ϵ_{static}

$$\epsilon_{static} = 1.0 - \frac{\text{apparent density}}{\text{non-porous density}} \qquad (D.1)$$

$$\epsilon_{static} = 1.0 - \frac{92.0}{169.0}$$

$$\epsilon_{static} = 0.457$$

Weight Mean Diameter, D_p

$$D_p = \sum wd \qquad (D.2)$$

where w is the weight percentage of particles of average sieve diameter d. Utilizing the data of Table 6,

$$D_p = 0.101(0.047) + 0.67(0.0272) + 0.225(0.0176) + 0.004(0.013)$$

$$D_p = 0.027 \text{ in.}$$

Effective Surface Area, S'''

$$S''' = \left(\frac{\alpha_s}{\alpha_v}\right) \sum \frac{w}{d} \qquad (D.3)$$

$$S''' = 0.01(6.1)\left[\frac{10.1}{0.047} + \frac{67.0}{0.0272} + \frac{22.5}{0.0176} + \frac{0.4}{0.013} \right] \quad (12)$$

$$S''' = 2,980 \text{ sq. ft./cu. ft.}$$

Table 7. Properties of Dry Air at Atmospheric Pressures (14.7 lb/sq.in.)

Temperature t °F	Density ρ $lb_m/ft.^3$	Dynamic Viscosity μ $lb_m/hr.ft.$	Kinematic Viscosity $ft.^2/hr.$	Specific Heat c_p $B/lb_m F$	Thermal Conductivity k B/hr.ft.F	Thermal Diffusivity α $ft.^2/hr.$	Prandtl Number N_{Pr}
- 100	0.1103	0.0324	0.294	0.2395	0.0107	0.405	0.726
- 80	045	338	323	95	112	447	23
- 60	0.0993	352	355	96	117	492	21
- 40	946	366	387	96	122	538	19
- 20	903	380	421	97	127	587	17
0	0.0864	0.0394	0.456	0.2397	0.0132	0.637	0.716
20	828	408	493	98	137	690	15
40	795	421	530	99	141	739	14
60	764	434	568	0.2400	146	796	13
80	736	447	607	02	151	854	12
100	0.0710	0.0460	0.649	0.2403	0.0155	0.909	0.711
120	685	473	691	05	160	971	10
140	662	485	733	06	165	1.036	09
160	641	497	775	08	169	095	08
180	621	508	818	11	173	156	07
200	0.0602	0.0520	0.864	0.2413	0.0178	1.225	0.706
220	584	532	911	16	182	290	05
240	568	543	956	19	186	354	04
260	552	554	1.004	22	191	429	03
280	537	565	052	25	195	498	02
300	0.0523	0.0576	1.101	0.2429	0.0199	1.567	0.703
320	509	588	155	32	203	640	04
340	497	599	205	36	207	709	05
360	485	610	258	41	211	782	05
380	474	620	308	46	215	855	05
400	0.0463	0.0631	1.363	0.2450	0.0219	1.931	0.705
420	452	641	418	55	223	2.009	06
440	442	651	473	69	227	088	06
460	432	661	530	66	231	169	06

Note: Values of N_{Pr} are smoothed.

```
COMMENT LEIGHTON E. SISSOM, SCHOOL OF M. E., EX. 452, APRIL 1965
        TEMPERATURE DISTRIBUTION OF SOLIDS AND PARTICLES IN FLUID TO
        PARTICLE HEAT TRANSFER IN A VERTICAL DUCT                          $
MONITOR ALPHA,BETA,ETA,LAMBDA,P,Q,R,A,B,DIS,PHI                            $
LOOP.. READ($$DATA)                                                        $
        WRITE($$TITLE0)                                                    $
        WRITE($$FLOWCONDITIONS,STYLE1)                                     $
        ALPHA=((EPSILON).(KF))/((1.0-EPSILON).(KSE))                       $
        BETA=-(GS.CS)/KSE                                                  $
        ETA=-((GF0).(CPF))/((1.0-EPSILON).(KSE))                           $
        LAMBDA=((H).(S))/((1.0-EPSILON).(KSE))                             $
        P=BETA+ETA/ALPHA                                                   $
        Q=-(LAMBDA.(ALPHA+1.0)-BETA.ETA)/ALPHA                             $
        R=-(LAMBDA.(BETA+ETA))/ALPHA                                       $
        A=Q-(P*2.0)/3.0                                                    $
        B=(2.0)(P*3.0)/27.0-P.Q/3.0+R                                      $
        DIS=(B*2.0)/4.0+(A*3.0)/27.0                                       $
        PHI=ARCCOS(-(B/2.0)/(SQRT(-A*3.0/27.0)))                           $
        M1=(2.0).(SQRT(-A/3.0)).COS(PHI/3.0)-P/3.0                         $
        M2=(2.0)(SQRT(-A/3.0)).COS(PHI/3.0+2.08)-P/3.0                     $
        M3=(2.0)(SQRT(-A/3.0)).COS(PHI/3.0+4.16)-P/3.0                     $
        F=1.0-(M1*2.0)/LAMBDA-(BETA.M1)/LAMBDA                             $
        F=1.0-(M2*2.0)/LAMBDA-(BETA.M2)/LAMBDA                             $
        G=1.0-(M3*2.0)/LAMBDA-(BETA.M3)/LAMBDA                             $
        WRITE($$TITLE1)                                                    $
        WRITE($$TITLE2)                                                    $
        LE=0.000                                                           $
TRIAL1.. LE=LE+0.001                                                       $
        J=EXP(M1.LE)                                                       $
        K=EXP(M2.LE)                                                       $
        N=EXP(M3.LE)                                                       $
        U=M1.EXP(M1.LE)                                                    $
        V=M2.EXP(M2.LE)                                                    $
        W=M3.EXP(M3.LE)                                                    $
```

```
        D=(J.V.G.W)+(K.W.E.U)+(N.U.F.V)-(N.V.E.U)-(K.U.G.W)-(J.W.F.V)
        -(E.V.G.W)-(F.W.E.U)-(G.U.F.V)+(G.V.E.U)+(F.U.G.W)+(E.W.F.V)   $
        D5=(TFIN).((J.V.G.W)+(K.W.E.U)+(U.F.V.N)-(N.V.E.U)-(K.U.G.W)
        -(J.W.F.V))-(TSIN).((E.V.G.W)+(F.W.E.U)+(U.F.V.G)-(G.V.E.U)
        -(F.U.G.W)-(E.W.F.V))                                          $
        D6=(TSIN.V.G.W)-(TSIN.W.F.V)-(TFIN.V.G.W)+(TFIN.W.F.V)         $
        D7=(TSIN.W.E.U)-(TSIN.U.G.W)-(TFIN.W.E.U)+(TFIN.U.G.W)         $
        D8=(TSIN.U.F.V)-(TSIN.V.E.U)-(TFIN.U.F.V)+(TFIN.V.E.U)         $
        C5=D5/D                                                        $
        C6=D6/D                                                        $
        C7=D7/D                                                        $
        C8=D8/D                                                        $
        TSLE=C5+C6.EXP(M1.LE)+C7.EXP(M2.LE)+C8.EXP(M3.LE)+0.1          $
        TFLE=C5+C6.E.EXP(M1.LE)+C7.F.EXP(M2.LE)+C8.G.EXP(M3.LE)        $
        IF (TFLE-TSLE GTR 0.0) AND (LE LSS L)                          $
        GO TO TRIAL1                                                   $
        LE=LE-0.001                                                    $
TRIAL2.. LE=LE+0.0001                                                  $
        J=EXP(M1.LE)                                                   $
        K=EXP(M2.LE)                                                   $
        N=EXP(M3.LE)                                                   $
        U=M1.EXP(M1.LE)                                                $
        V=M2.EXP(M2.LE)                                                $
        W=M3.EXP(M3.LE)                                                $
        D=(J.V.G.W)+(K.W.E.U)+(N.U.F.V)-(N.V.E.U)-(K.U.G.W)-(J.W.F.V)
        -(E.V.G.W)-(F.W.E.U)-(G.U.F.V)+(G.V.E.U)+(F.U.G.W)+(E.W.F.V)   $
        D5=(TFIN).((J.V.G.W)+(K.W.E.U)+(U.F.V.N)-(N.V.E.U)-(K.U.G.W)
        -(J.W.F.V))-(TSIN).((E.V.G.W)+(F.W.E.U)+(U.F.V.G)-(G.V.E.U)
        -(F.U.G.W)-(E.W.F.V))                                          $
        D6=(TSIN.V.G.W)-(TSIN.W.F.V)-(TFIN.V.G.W)+(TFIN.W.F.V)         $
        D7=(TSIN.W.E.U)-(TSIN.U.G.W)-(TFIN.W.E.U)+(TFIN.U.G.W)         $
        D8=(TSIN.U.F.V)-(TSIN.V.E.U)-(TFIN.U.F.V)+(TFIN.V.E.U)         $
        C5=D5/D                                                        $
        C6=D6/D                                                        $
```

```
        C7=D7/D                                                          $
        C8=D8/D                                                          $
        TSLE=C5+C6.EXP(M1.LE)+C7.EXP(M2.LE)+C8.EXP(M3.LE)+0.1            $
        TFLE=C5+C6.E.EXP(M1.LE)+C7.F.EXP(M2.LE)+C8.G.EXP(M3.LE)          $
        IF (TFLE-TSLE GTR 0.0) AND (LE LSS L)                            $
        GO TO TRIAL2                                                     $
        LE=LE-0.0001                                                     $
TRIAL3.. LE=LE+0.00001                                                   $
        J=EXP(M1.LE)                                                     $
        K=EXP(M2.LE)                                                     $
        N=EXP(M3.LE)                                                     $
        U=M1.EXP(M1.LE)                                                  $
        V=M2.EXP(M2.LE)                                                  $
        W=M3.EXP(M3.LE)                                                  $
        D=(J.V.G.W)+(K.W.E.U)+(N.U.F.V)-(N.V.E.U)-(K.U.G.W)-(J.W.F.V)
        -(E.V.G.W)-(F.W.E.U)-(G.U.F.V)+(G.V.E.U)+(F.U.G.W)+(E.W.F.V)      $
        D5=(TFIN).((J.V.G.W)+(K.W.E.U)+(U.F.V.N)-(N.V.E.U)-(K.U.G.W)
        -(J.W.F.V))-(TSIN).((E.V.G.W)+(F.W.E.U)+(U.F.V.G)-(G.V.E.U)
        -(F.U.G.W)-(E.W.F.V))                                            $
        D6=(TSIN.V.G.W)-(TSIN.W.F.V)-(TFIN.V.G.W)+(TFIN.W.F.V)           $
        D7=(TSIN.W.E.U)-(TSIN.U.G.W)-(TFIN.W.E.U)+(TFIN.U.G.W)           $
        D8=(TSIN.U.F.V)-(TSIN.V.E.U)-(TFIN.U.F.V)+(TFIN.V.E.U)           $
        C5=D5/D                                                          $
        C6=D6/D                                                          $
        C7=D7/D                                                          $
        C8=D8/D                                                          $
        TSLE=C5+C6.EXP(M1.LE)+C7.EXP(M2.LE)+C8.EXP(M3.LE)+0.1            $
        TFLE=C5+C6.E.EXP(M1.LE)+C7.F.EXP(M2.LE)+C8.G.EXP(M3.LE)          $
        IF (TFLE-TSLE GTR 0.0) AND (LE LSS L)                            $
        GO TO TRIAL3                                                     $
        WRITE($$OUT1,FMT1)                                               $
COMMENT THIS COMPLETES THE TRIAL AND ERROR PROCESS AND DETERMINES THE
        EFFECTIVE LENGTH.  THE PARAMETERS FOR THIS EFFECTIVE LENGTH
        ARE NOW GIVEN                                                    $
```

```
        WRITE($$TITLE3)                                                    $
        WRITE($$TITLE4)                                                    $
        FOR X=(1.0,0.001,LE+1.0)                                           $
BEGIN   Z=X-1.0                                                            $
        TS=C5+C6.EXP(M1.Z)+C7.EXP(M2.Z)+C8.EXP(M3.Z)                       $
        TF=C5+C6.E.EXP(M1.Z)+C7.F.EXP(M2.Z)+C8.G.EXP(M3.Z)                 $
        WRITE($$TEMPERATUREFIELD,FMT2)          END                        $
COMMENT THIS GIVES THE TEMPERATURE DISTRIBUTION FOR THE THEORETICAL
        EFFECTIVE LENGTH FOR ONE SET OF INPUT DATA                         $
        GO TO LOOP                                                         $
FORMAT  TITLE0(B3,*GF0*,B7,*CPF*,B8,*GS*,B8,*CS*,B5,*EPSILON*,B6,*KF*,
        B8,*H*,B9,*S*,B8,*KSE*,B8,*L*,B8,*TSIN*,B6,*TFIN*,W3)              $
OUTPUT  FLOWCONDITIONS(GF0,CPF,GS,CS,EPSILON,KF,H,S,KSE,L,TSIN,TFIN)       $
FORMAT  STYLE1(B1,X8.3,B3,X4.2,B3,X11.2,B4,X4.3,B6,X4.3,B5,X5.3,B5,
        X6.3,B3,X6.1,B5,X6.3,B4,X4.2,B5,X7.2,B3,X7.2,W4)                   $
FORMAT  TITLE1(B21,*PARAMETERS FOR THE TEMPERATURE DISTRIBUTION IN FLUI
D TO PARTICLE HEAT EXCHANGE*,W4)                                           $
FORMAT  TITLE2(B6,*M1*,B10,*M2*,B10,*M3*,B10,*E*,B11,*F*,B11,*G*,B11,
        *C5*,B10,*C6*,B10,*C7*,B10,*C8*,W4)                                $
FORMAT  TITLE3(B30,*TEMPERATURE DISTRIBUTION IN FLUID TO PARTICLE HEAT
EXCHANGE*,W4)                                                              $
FORMAT  TITLE4(B43,*Z*,B14,*TS*,B15,*TF*,W4)                               $
INPUT   DATA(GF0,CPF,GS,CS,EPSILON,KF,H,S,KSE,L,TSIN,TFIN)                 $
OUTPUT  OUT1(M1,M2,M3,E,F,G,C5,C6,C7,C8)                                   $
FORMAT  FMT1(B1,F10.4,9(B2,F10.4),W4)                                      $
OUTPUT  TEMPERATUREFIELD(Z,TS,TF)                                          $
FORMAT  FMT2(B40,X5.3,2(B11,X7.2),W4)                                      $
        FINISH                                                             $
```

LITERATURE CITED

1. M. Jakob, Heat Transfer, Vol. II, John Wiley and Sons, Inc., New York, N. Y., 1963, p. 268ff.

2. W. Cramp and A. Priestley, "Pneumatic Grain Elevators," The Engineer, 139, 1924, p. 89.

3. H. Chatley, "The Pumping of Granular Solids in Fluid Suspensions," Engineering, 149, 1940, p. 230.

4. R. F. Davis, "The Conveyance of Solid Particles by Fluid Suspension," Engineering, 140, 1935, p. 1.

5. R. C. Worster and D. F. Denny, "Hydraulic Transport of Solid Material in Pipes," Institution of Mechanical Engineers, 169, 1955, p. 563.

6. D. M. Newitt, J. F. Richardson, M. Abbott, and R. B. Turtle, "Hydraulic Conveying of Solids in Horizontal Pipes," Transactions Institution of Chemical Engineers, 33, 1955, p. 93.

7. B. J. Gliddon, "The Hydraulic Transport of Solids in Vertical Pipe-Lines," Journal of the Imperial College Chemical Engineering Society, 11, 1957, p. 152.

8. L. Lapidus and J. C. Elgin, "Mechanics of Vertical-Moving Fluidized Systems," American Institute of Chemical Engineers Journal, 3, 1957, p. 63.

9. B. G. Price, L. Lapidus, and J. C. Elgin, "Mechanics of Vertical Moving Fluidized Systems: II. Application of Countercurrent Operation," AIChE J., 5, 1959, p. 93.

10. D. L. Struve, L. Lapidus, and J. C. Elgin, "The Mechanics of Moving Vertical Fluidized Systems: III. Application to Cocurrent Countergravity Flow," Canadian Journal of Chemical Engineering, 36, 1958, p. 141.

11. R. F. Hoffman, L. Lapidus, and J. C. Elgin, "The Mechanics of Vertical Moving Fluidized Systems: IV. Application to Batch-Fluidized Systems with Mixed Particle Sizes," AIChE J., 6, 1960, p. 321.

12. J. A. Quinn, L. Lapidus, and J. C. Elgin, "The Mechanics of Moving Vertical Fluidized Systems: V. Concurrent Cogravity Flow," AIChE J., 7, 1961, p. 260.

13. J. W. Delaplaine, "Forces Acting in Flowing Beds of Solids," AIChE J., 2, 1956, p. 127.

14. A. W. Jenike, "Gravity Flow of Bulk Solids," Bulletin of the University of Utah: Bulletin No. 108, Vol. 52, No. 29, 1961.

15. A. W. Jenike, "Gravity Flow of Bulk Solids," Trans. Instn. Chem. Engrs., 40, 1962, p. 264.

16. F. A. Zenz and D. F. Othmer, Fluidization and Fluid-Particle Systems, Reinhold Publishing Corp., New York, N. Y., 1960.

17. Proceedings of the Symposium on the Interaction Between Fluids and Particles, London, Institution of Chemical Engineers, June 1962.

18. S. Yagi and N. Wakao, "Heat and Mass Transfer from Wall to Fluid in Packed Beds," AIChE J., 5, No. 1, 1959, p. 79.

19. K. N. Kettenring, E. L. Manderfield, and J. M. Smith, "Heat and Mass Transfer in Fluidized Systems," Chemical Engineering Progress, 46, No. 3, 1950, p. 139.

20. E. Singer and Richard Wilhelm, "Heat Transfer in Packed Beds," Chem. Eng. Prog., 46, No. 7, 1950, p. 343.

21. S. Yagi, D. Kunii, and K. Endo, "Heat Transfer in Packed Beds Through Which Water is Flowing," International Journal of Heat and Mass Transfer, 7, 1964, p. 333.

22. J. Frantz, "Fluid-to-Particle Heat Transfer in Fluidized Beds," Chem. Eng. Prog., 57, No. 7, 1961, p. 35.

23. H. Fujishige, "Heat Transfer Between Wall and Fluidized Bed," Kagaku-Kogaku (Journal of the Chemical Society of Japan), 67, No. 9, 1964, p. 1316.

24. H. Fujishige, "Heat Transfer Between Particles and Air in Fluidized Bed," J. Chem. Soc. of Japan, 67, No. 9, 1964, p. 1322.

25. D. Kunii, "Heat Transfer in Powdery or Granular Materials," J. Chem. Soc. of Japan, 25, 1961, p. 891.

26. S. Yagi and D. Kunii, "Studies on Effective Thermal Conductivities in Packed Beds," AIChE J., 3, 1957, p. 373.

27. R. Gorring and S. W. Churchill, "Thermal Conductivity of Heterogeneous Materials," Chem. Eng. Prog., 57, 1961, p. 53.

28. R. Bernard and R. Wilhelm, "Turbulent Diffusion in Fixed Beds of Packed Solids," Chem. Eng. Prog., 46, No. 5, 1950, p. 233.

29. W. Munro and N. Amundson, "Solid-Fluid Heat Exchange in Moving Beds," Industrial and Engineering Chemistry, 42, No. 8, 1950, p. 1481.

30. F. Zenz, Fluidization and Fluid-Particle Systems, Reinhold Publishing Corp., New York, N. Y., 1960.

31. M. Leva, Fluidization, McGraw-Hill Book Co., Inc., New York, N. Y., 1959.

32. J. DallaValle, Micromeritics, Pitman Publishing Corp., New York, N. Y., 1943, p. 49ff.

33. A. London, "Compact Heat Exchangers," Mechanical Engineering, 86, No. 5, 1964, p. 47.

34. J. Francl and W. D. Kingery, "Thermal Conductivity: IX, Experimental Investigation of Effect of Porosity on Thermal Conductivity," Journal of the American Ceramic Society, 37, 1954, p. 99.

35. D. Kunii and J. M. Smith, "Heat Transfer Characteristics of Porous Rocks," AIChE J., 6, 1960, p. 71.

OTHER REFERENCES

Bird, R. B., Stewart, W. E., and E. N. Lightfoot, Transport Phenomena, John Wiley and Sons, Inc., 1962.

Caldas, Isidoro, Jr., Heat Transfer to Fluidized Beds, PhD Thesis, University of Cincinnati, 1955.

Chechetkin, A., High Temperature Heat Carriers, Pergamon Press, New York, N. Y., 1963.

Ellis, H. S., Redberger, P. J., and L. H. Bolt, "Transporting Solids: Slurries, Basic Principles and Power Requirements," Ind. Eng. Chem., 55, 1963, p. 18.

Happel, J., "Pressure Drop Due to Vapor Flow Through Moving Beds," Ind. Eng. Chem., 41, 1949, p. 1161.

Hryniszak, W., Heat Exchangers, Academic Press, Inc., New York, N. Y., 1958.

Jakob, M., Heat Transfer, Vol. I, John Wiley and Sons, Inc., New York, N. Y., 1962.

Kays, W. and A. London, Compact Heat Exchangers, McGraw-Hill Book Co., Inc., New York, N. Y., 1964.

Loeffler, A. L., Jr. and B. F. Ruth, "Particulate Fluidization and Sedimentation of Spheres," AIChE J., 5, 1959, p. 310.

McAdams, W., Heat Transmission, 3rd Ed., McGraw-Hill Book Co., Inc., New York, N. Y., 1954.

Scheidegger, A. E., The Physics of Flow Through Porous Media, The Macmillan Co., New York, N. Y., 1957.

Thomas, D. G., "Flow of Non-Newtonian Suspensions," Ind. Eng. Chem., 55, 1963, p. 18ff.

Ting, A. P. and R. H. Luebbers, "Viscosity of Suspensions of Spherical and Other Isodimensional Particles in Liquids," AIChE J., 3, 1957, p. 111.

Yagi, S. and W. Noriaki, "Heat and Mass Transfer from Wall to Fluid in Packed Beds," AIChE J., 5, 1959, p. 79.

VITA

Leighton Esten Sissom was born in Coffee County, Tennessee on August 26, 1934. He attended the public schools of Coffee County graduating from Central High School, Manchester, Tennessee in May 1961. He entered Middle Tennessee State College in the same year and received a Bachelor of Science degree in Industrial Arts in 1956 after a brief respite while employed by Chrysler Corporation and part-time employment with Westinghouse Electric Corporation. He then went into mechanical design with Westinghouse and ARO, Inc. where he remained until September 1958. At that time he became an Instructor in the Engineering Science Department of Tennessee Polytechnic Institute while attending classes part-time in the Mechanical Engineering Department. He was graduated with a degree of Bachelor of Science in Mechanical Engineering in 1962. He then entered the Georgia Institute of Technology where he received a degree of Master of Science in Mechanical Engineering in 1964 and continued to pursue the Doctor of Philosophy in the School of Mechanical Engineering.

Mr. Sissom was married in 1953 to the former Evelyn Janelle Lee. They have two sons, Terry Lee and Denny Leighton.